1-1-2017

Towards a Better Understanding of Secondary Metabolite Production in Toxic Marine Algae

Thuy My Nguyen
University of Mississippi

TOWARDS A BETTER UNDERSTANDING OF SECONDARY METABOLITE PRODUCTION IN TOXIC MARINE ALGAE

A Thesis

Presented in partial fulfillment of requirements

for the degree of Master of Science

in the Department of Biology

The University of Mississippi

By:

THUY M. NGUYEN

August 2017

ABSTRACT

Roseofilum reptotaenium is a marine cyanobacteria responsible for the loss of 50% of corals worldwide due to Black Band Disease (BBD). Investigating the basis for secondary metabolite production by *R. reptotaenium* cultures revealed a suite of potent anti-malarial and anticancer compounds that likely include dolastatin 10 and monomethyl auristatin D (MMAD). These *R. reptotaenium* cultures are non-axenic (not pure monocultures) and *R. reptotaenium* appears to require the presence of several heterotrophic bacteria to survive. Scanning Election Microscope (SEM) images show closely associated bacteria. Preliminary metagenomic analysis indicates three dominant non-cyanobacterial phyla: Bacteroidetes, Planctomycetes, and Proteobacteri (α-proteobacteria accounted for >50% of the entire community). We are explored the role of these bacteria with *R. reptotaenium* in producing the complex of dolastatin/MMAD compounds, seeking to understand the chemical ecology and genetic basis by which these compounds are produced. The potential involvement of the dolastatin-like suite of compounds in Black Band Disease in corals merits further study given the destructiveness of this disease on corals worldwide.

ACKNOWLEDGEMENTS

I would like to thank Dr. Erik Hom for his guidance in all aspects and stages of this thesis project. I would also like to thank Drs. Gregg Roman and Marjorie Holland for their advice in improving this project and the final thesis. I thank Dr. Amar Chittiboyina, Dr. Yang-Hong Wang for LC-MS/MS and chemical/structural analysis of compounds in the active fractions, Dr. Melissa Jacob for general bioactivity testing, Dr. David Pasco for anti-cancer assays, and Dr. Colin Jackson for preliminary metagenomic analysis of *R. reptotaenium* cultures, Dr. Sarah Lijigren and Dr. Patrick Curtis for use of chemicals in a pinch. I would like to thank Dr. Michael Lomas and Dr. Julie Sexton for providing *R. reptotaenium* cultures and valuable help with algal culturing techniques. I would also like to thank the Vietnam Education Foundation and the Hannah T. Croasdale Fellowship program (of the Phycological Society of America) for providing me with financial support and opportunities to pursue my research interests. I would also like to thank Dr. Tammy Goulet and Mark McCauley for collaborating on the coral experiments described. Lastly, I thank Sean Moyer, Holly Prather, Michael Clear, Victoria Calatrava, Jessica Marshall, and Kirby Thomas for their encouragement and assistance with lab work.

TABLE OF CONTENTS

LIST OF FIGURES

LIST OF TABLES

INTRODUCTION

Coral reefs cover about 600,000 square kilometers of the Earth's surface (Crossland et al. 1991), and are among the most diverse biological ecosystems in the world (Lesser et al. 2007). Coral reefs provide several important physical, biological, and cultural services (Cesar 2002). They serve as a habitat for many different marine organisms, thereby maintaining biodiversity (Cesar 2002). They are also a tremendous source of marine products (e.g., seafood, raw materials, jewelry, and medicinal compounds), which are valued at approximately $375 billion per year (Richardson 1998).

Coral reef ecosystems have been degraded at an alarming rate because of the impact of several threats derived from human activity (e.g., over-exploitation in fishing, non-sustainable tourism practices, and pollution) and natural factors (e.g., tropical storms, climatic changes, and coral diseases) (Lesser et al. 2007). Coral diseases are considered a major cause of coral reef loss. A survey of coral reef diseases in Florida Keys reef in 2001 showed that the number of locations exhibiting coral disease increased by 80%, and the the rate of coral mortality increased by 60% compared to data from 1996 (Santavy et al. 2001). Black band disease (BBD) is one of six dominant coral diseases infecting reefs globally and contributes to 50% of the loss of corals by the disease (Harborne et al. 2006; Harvell et al. 2001; Peters 1984).

Black Band Disease (BBD) is marked by dense black bands or rings that circumscribe regions of damaged coral tissue (Garzón et al. 2001), and has been show to be caused by the marine cyanobacterium *Roseofilum reptotaeneum* (Fig.1). BBD was first observed on stony

corals in the Caribbean in the 1970s (Antonius 1977), but is now found on tropical and subtropical coral reefs worldwide (Sutherland et al 2004). BBD is a seasonal disease, with high prevalence when the temperature is above 29-30°C (Richardson et al. 2014). BBD can progress at a rate of 0.3 - 1 cm per day, and can kill a coral colony over several months.

Figure 1. *R. reptotaenium* (left) causes Black Band Disease (see red arrow) in corals (Scale bar of *R. reptotaenium* filaments is 10 μm)

According to Richardson's hypothesis (2014), BBD is caused by the synergistic action of microcystin toxin produced by *R. reptotaenium* and hydrogen sulfide produced by sulfate reducing bacteria (Richardson et al. 2014). These conditions are believed to kill the symbionts (*Symbiodinium* sp.) living in corals, leading to bleaching and coral degradation. Coral bleaching is the phenomenon that happens when the symbiotic interaction between coral hosts and symbionts is disrupted; corals will lose their algae symbionts and algal photosynthetic pigments, then turn to white color (Correa et al. 2009). *Symbiodinium* is the dinoflagellate living in symbiosis with corals and their relatives (Pochon et al. 2006). Corals provide a safe environment and the necessary compounds for *Symbiodinium*'s photosynthetic process while *Symbiodinium* supplies photosynthetically fixed carbon (sugars, and lipids) back to corals (Correa et al. 2009; Kirk et al. 2005). The sea anemone *Aiptasia* (Fig. 2) is a genus of symbiotic cnidarian in the

Anthozoa class, and also lives in symbiosis with *Symbiodinium* sp. The symbiosis relationship between *Aiptasia* and *Symbiodinium* sp. is similar to the relationship between corals and *Symbiodinium* sp., and *Aiptasia* is often used as a laboratory model to for corals, given the endangered nature of many corals.

Figure 2. The sea anemone *Aiptasia sp*. isolated from Florida Keys and cultivated in the laboratory.

Richardson demonstrated that *R. reptotaenium* cultures can cause BBD-like symptoms on *Diploria strigosa* stony coral fragments after 7 days of cultivation in the laboratory; after 28 days, the coral skeleton completely disintegrated (Richardson et al. 2014). However, exposure of healthy coral fragments to microcystin at concentrations of 50-100 μM did not appear to injure the coral and only resulted in a decreased number of heterotrophic bacteria on the coral surface (Richardson et al. 2009). *R. reptotaenium* is a phycoerythrin (brownish-red), motile, unbranched filamentous cyanobacterium first classified as *Oscillatoria submembranaceae* (1981) and then as *Phormidium corallyticum* (1983) based on morphology. In 2009, these were re-classified as *Pseudoscillatoria coralii* based on 97% sequence similarity (Rasoulouniriana et al. 2009). However, *Pseudoscillatoria coralii* is a dark blue-green algae with phycocyanin, not phycoerythrin, the pigment dominant in the brownish-red algae. Taxonomic revisions in 2012 by

Casamatta re-classified these as *Roseofilum reptotaenium* and further demonstrated in the laboratory that *R. reptotaenium* was the causative agent of BBD (Casamatta et al. 2012). A *R. reptotaenium* type strain has been deposited at the National Center for Marine Algae and Microbiota (NCMA) (at the Bigelow Laboratory for Ocean Sciences) and maintained as CCMP3313, which is the culture source for the work described in this thesis.

R. reptotaenium grows filamentously, with filaments about 3.0-3.9 μm wide and an average cell length of 2.5-4.0 μm. *R. reptotaenium* can grow photoautotrophically or mixotrophically, but not heterotrophically (Richardson 2003). The *R. reptotaenium* cultures are non-axenic (i.e., not pure monocultures) and *R. reptotaenium* appears to require the presence of several heterotrophic bacteria to survive. *R. reptotaenium* experiences the highest growth rate on L1 salt water medium in comparison to ASNIII, F2, and IMK culture media (Buerger et al. 2016). *R. reptotaenium* exhibits clumping behavior and grows faster in non-disturbed conditions than in stirred or agitated culture conditions (Richardson et al. 2014). Clumping behavior is believed to lead to self-shading and reduced exposure to high intensity light (Castenholz 1988).

In 2011, it was determined through enzyme-linked immunosorbent assay (ELISA) tests that *R. reptotaenium* cultures produce the cytotoxin microcystin-LR at a concentration of 20-40 $\mu g\ g^{-1}$ biomass (Stanić et al. 2011). Microcystins (MC) are a group of cyclic heptapeptide toxins produced by the cyanobacterial genera *Microcystis, Oscillatoria, Planktothrix, Anabaena, and Nostoc* (Niedermeyer et al. 2012). MCs contain 80 structural variants with the general structure cyclo-(D-alanine^{1}- X^{2}-D-MeAsp^{3}-Z^{4}-Adda^{5}-D-glutamate^{6}-Mdha^{7}), where X and Z represent two variable L-amino acids (Fig. 3-left) (Sheng et al. 2007). Microcystin-LR (MC-LR) is the most toxic variant in which the two variable L-amino acids are leucine and arginine (Fig. 3-right) (MacKintosh et al. 1990). Microcystin-contaminated drinking water represents a serious human

health risk due to the damaging liver effects of microcystins once consumed (Hooser 2000; MacKintosh et al. 1990; Falconer et al. 1981). Microcystins can also act as tumor promoters, causing liver cancer (Hooser 2000). Experimentally, it has been shown to directly damage the livers of rat and mice after a few minutes of exposure (Falconer et al. 1981).

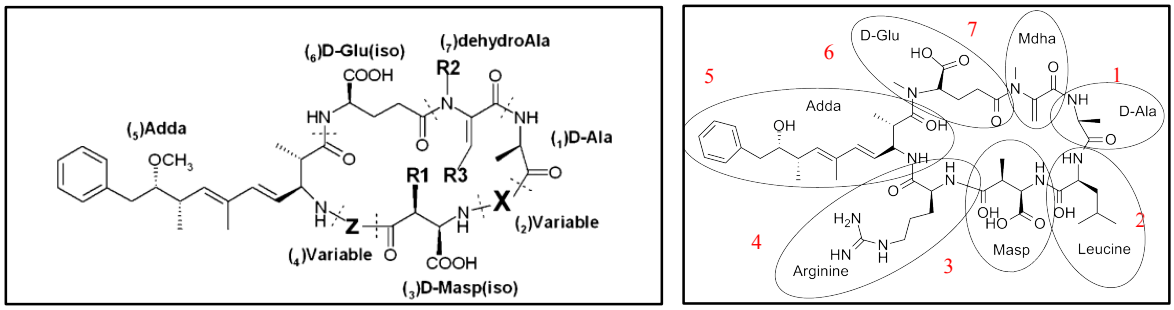

Microcystins **Microcystins LR**

Figure 3. Molecular structure of Microcystins and Microcystin LR

In 2007, studies were initiated with MC-LR to determine its potential as an anticancer compound on the basis of two characteristics (Monks et al. 2007). Firstly, MC-LR is only toxic after being absorbed into liver cells due to its poor membrane permeability (Monks et al. 2015). Secondly, MC-LR kills cancer cells through phosphatase inhibition, but *not* by inducing apoptosis (Monk et al. 2015). Therefore, MC-LR can work effectively against apoptosis-resistant cancer cell lines. The action of microcystins against cancer cells is based on the activity of organic anion transporting polypeptides (OATP) (Daily et al. 2010; König et al. 2006). OATP-1B1 and OATP-1B3 are two human proteins that can mediate the transport of microcystins from blood to liver cells. OATP-1B1 is fairly abundant in liver tissues while OATP-1B3 is more widely distributed in liver cancer cells than in healthy cells (Monk et al. 2015). The selectivity that favors OATP-1B3 over OATP-1B1 can offer a therapeutic window for the respective compound (Monk et al. 2015; Monks et al. 2007; Sainis et al. 2010).

In 2012, two hundred and seven algal cultures were sent from the Bigelow laboratory/NCMA to the National Center of Natural Products Research (NCNPR) for bioactivity screenings. The preliminary data suggested that *R. reptotaenium* cultures might possess potent antimalarial activity. While promising, the materials sent (15 mL of liquid culture per algal strain) were not sufficient for initiating follow-up experiments. *R. reptotaenium* also proved very difficult to culture under laboratory conditions by former research groups (Bigelow and Richardson labs). Owing to scientists at the NCNPR not having algal culturing expertise, research capacity, or sufficient interest to follow-up, this collaborative effort stalled for several years. From the start, the Hom lab was interested in collaborating with Dr. Michael Lomas at the Bigelow Laboratory to better understand the chemical and microbial ecology of algae within the NCMA culture collection. In 2015, I started working on studying several marine algal cultures before focusing on *R. reptotaenium*, given its relatively faster cell culturing times.

METHODS

R. reptotaenium culturing and extractions

Erlenmeyer flasks containing 1.5 L of L1 seawater medium (Guillard et al. 1993) (see recipe in Appendix A) were inoculated with 0.5-gram of wet *R. reptotaenium* biomass. Flasks were covered twice by multipurpose white paper (Georgia-Pacific Consumer Products, Atlanta, GA) and maintained at 30°C and 27 $\mu Em^{-2}s^{-1}$ under a 12:12 light/dark cycle of cool-white light. *R. reptotaenium* cultures were centrifuged at 2000 g for 3 minutes to separate biomass from supernatant for downstream secondary metabolite extraction (Fig. 4). As described in greater detail below, secondary metabolites present in the supernatant and the biomass were extracted by ethyl acetate and methanol, respectively, and solvent-evaporated to generate "crude" extracts. These crude extracts were further fractionated, dried down, resuspended in dimethylsulfoxide (DMSO), and submitted for antimalarial and anticancer assays, and chemical characterization (LC-MS/MS). DNA from fragments of biomass was also isolated for metagenomic 16S rDNA amplicon sequencing (Fig. 4).

Biomass extractions.

To extract secondary metabolites from *R. reptotaenium* cells, 300 mg of biomass was transferred to a 50 mL falcon containing 30 mL of methanol, and sonicated for 5 minutes at 400Hz using a Branson M1800 ultrasonic bath (Branson Ultrasonics, Dansbury, CT). The resulting methanol slurry was centrifuged at 22,000g for 3 minutes. The biomass pellet was then subjected to two more extractions with methanol. Methanol supernatants were pooled and

evaporated at 30°C for 20 minutes to generate what we refer to as "crude biomass extracts." Genomic DNA was isolated from two hundred mg of fresh *R. reptotaenium* biomass from 2 week-old and 8 week-old cultures. Genomic DNA was extracted using 500 μl of phenol: chloroform: isoamyl alcohol (25:24:1), cleaning up by 500 μl of isopropanol, precipitated overnight in 200 μl of ethanol, and re-dissolved in 20 μl TE buffer. The prokaryotic composition of *R. reptotaenium* cultures was characterized using a 250-bp portion of the bacterial 16S rRNA gene and Illumina MiSeq sequencing as previously described (Kozich et al. 2013; Jackson et al. 2015). Samples were pooled, spiked with 5 % PhiX (Jackson et al. 2015), and sequenced at the University of Mississippi Medical Center Molecular and Genomics Core Facility (courtesy of Dr. Colin Jackson). Raw sequences were analyzed by mothur 1.40.0 (Schloss et al. 2009, 2011). Sequences were aligned against the SILVA V4 16S rRNA database (Quast et al. 2013), and chimeras were detected using UCHIME (Edgar et al. 2011). Valid sequences were classified using the Greengenes 16S rRNA classification scheme (DeSantis et al. 2006), with chloroplast (and mitochondrial) sequence contaminants removed. Bacterial sequences were grouped into operational taxonomic units (OTUs) based on 97 % sequence similarity.

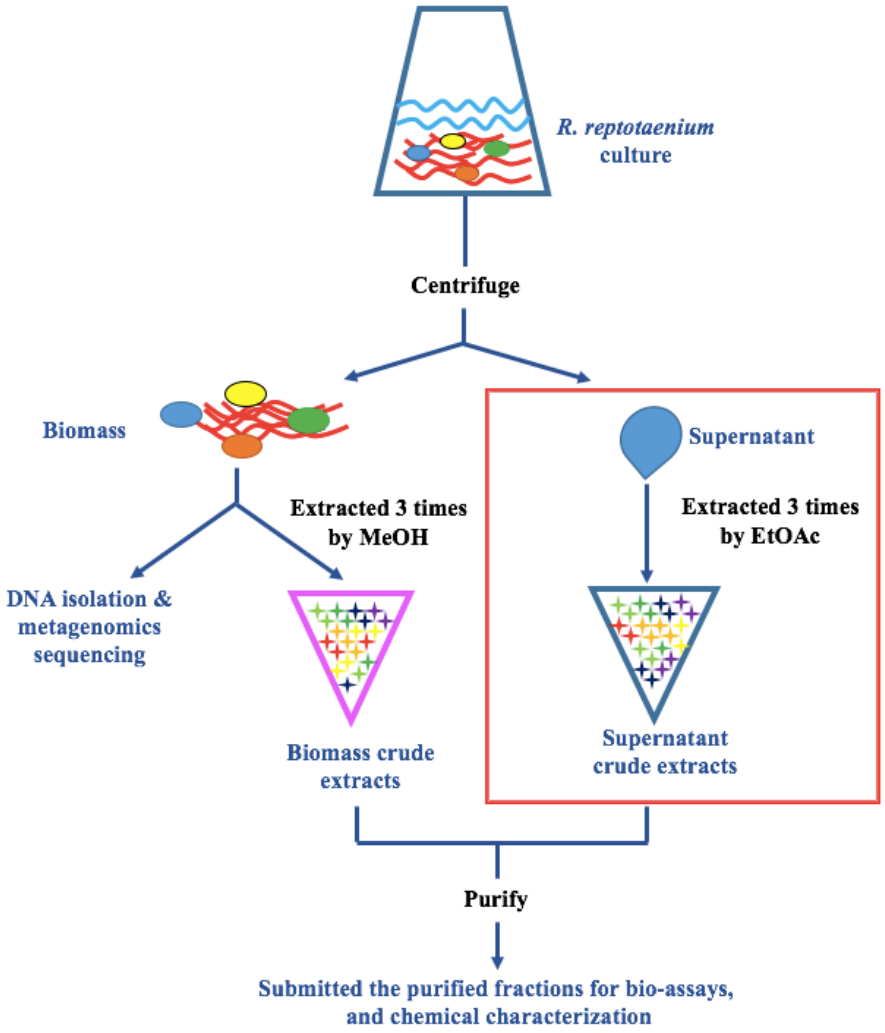

Figure 4. Protocol schematic for metabolite extraction from *R. reptotaenium* culture (The information in the red box is represented in Fig.5).

Supernatant extractions

The cell-clarified supernatant of *R. reptotaenium* cultures was transferred to a 1.5 L separatory funnel and combined with an equal volume of ethyl acetate (EtOAc) organic solvent. The funnel was inverted gently ten times in order to allow the partitioning of the active compounds into the EtOAc organic phase. After several minutes of allowing aqueous and organic phases to separate, the lighter EtOAc phase (density ~ 0.902 g/cm^3) was isolated to ensure that any trace amounts of water were removed, while the supernatant were subjected to

two more rounds of EtOAc extraction. EtOAc phases were combined and evaporated using a BUCHI rotovapor R100 rotary evaporator (BUCHI Corp., New Castle, DE) for 45 minutes at 30°C to generate what we refer to as "crude supernatant extracts" (Fig.5).

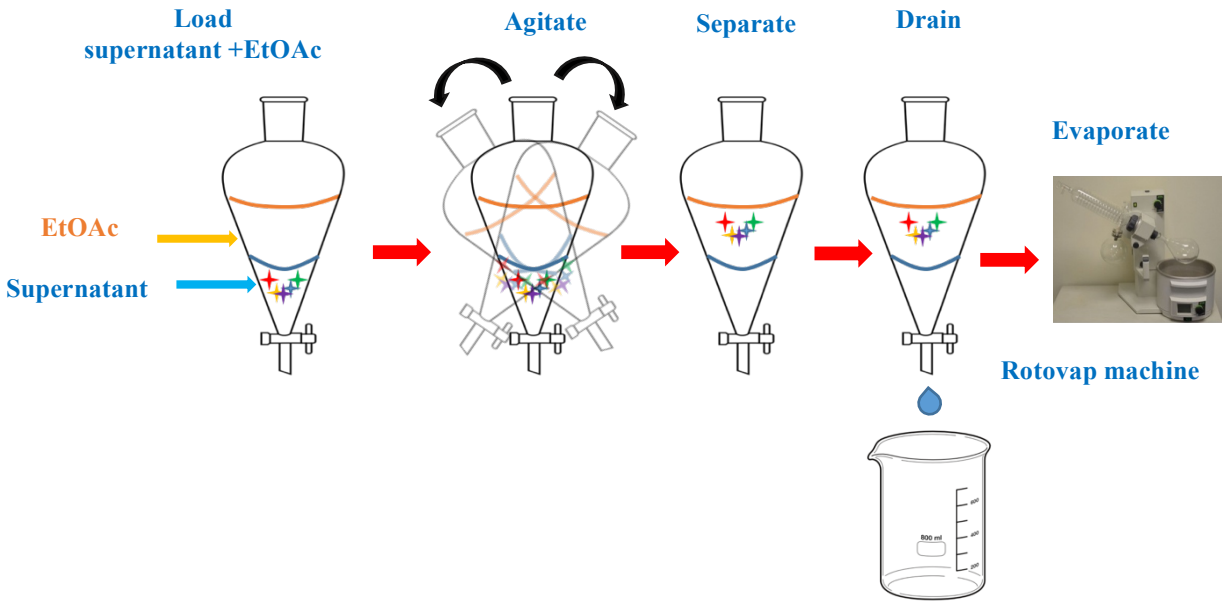

Figure 5. Protocol schematic for the generation of the crude extracts from the supernatant of the *R. reptotaenium* culture.

Purification of crude extracts by reverse phase chromatography.

Reverse-phase chromatography (RPC) is widely used in drug-discovery to purify potent compounds from crude extracts. RPC involves two parts, a non-polar hydrophobic stationary phase and a polar hydrophilic mobile phase. Due to the polar/non-polar chemistry of the mobile/stationary phases, polar compounds that do not interact with the surface of stationary phase are eluted first while the non-polar compounds are eluted last. The stationary phase usually contains a long alkyl chain, and we used a column with 18 carbons (C18); for the mobile phase, we used methanol (MeOH) or acetonitrile (CH_3CN), with CH_3CN being a slightly more polar solvent (Mantoura et al. 1983).

Crude extracts were dissolved in 1mL of 1:1 methanol: water and loaded onto a C18 column in 100 mg portions, and eluted by a series of six MeOH concentrations (0%, 20%, 40%, 60%, 80%, 100%), with a final elution using 100% acetone. These seven solvent fractions were individually dried by rotavap evaporation at 30°C for 5 min, dissolved in DMSO, and submitted for antimalarial and anticancer assays, and chemical characterization (LC-MS/MS) (Fig. 6)

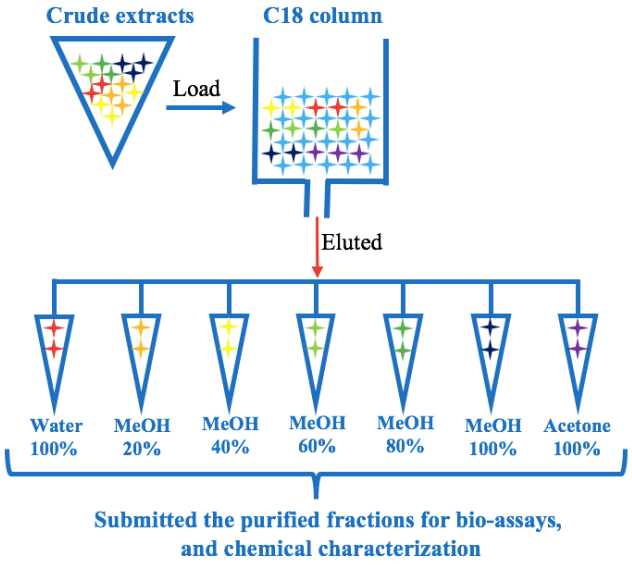

Figure 6. *R. reptotaenium* crude extracts (biomass and supernatant) were eluted by methanol (MeOH) at different concentration through the C18 column.

Similarly, 100 mg crude extracts dissolved in 1mL of 1: 1 methanol: water were loaded onto a C18 column and eluted by a series of six CH_3CN concentrations (0%, 20%, 40%, 60%, 80%, 100%), followed by 100% Acetone. These seven purified fractions were also submitted for antimalarial and anticancer assays, and chemical characterization (LC-MS).

Characterizing potent compounds in the crude extracts by LC-MS.

Liquid chromatography-mass spectrometry (LC-MS) is an analytical chemistry technique that combines the physical separation capabilities of high performance liquid chromatography (HPLC) and the mass analysis capabilities of mass spectrometry (MS) (Pitt 2009). HPLC is a

technique which forces a liquid solution (mobile phase) containing potential drug compounds into a C18 silica column (stationary phase) by high pressure. Due to varying polarities of the compounds present in the solution, there are time differences in elution of the compounds. MS is an analytical technique which is used to elucidate the chemical structures of molecules by determining the mass and elemental compositions of a given sample (Dass 2007). MS ionizes the molecules by an electron beam or UV light to produce charged molecules (ions). These ions are then separated by electromagnetic fields based on their mass-to-charge ratio (Dass 2007).

LC-MS/MS is similar to LC-MS except LC-MS/MS generates secondary MS fragmentations of the primary precursor ion. The advantages of MS/MS are increased sensitivity and the ability to provide more detailed structural information based on the sub-fragmentation patterns. In collaboration with Dr. Yan-Hong Wang (NCNPR), the active fractions identified in the antimalarial and anticancer assays were submitted for chemical characterization by LC-MS/MS (Waters ACQUITY UPLC system coupled with Xevo G2-S ToF mass spectrometer) using the gradient conditions shown below (Table 1).

Table 1. Gradient conditions used for LC-MS/MS analysis of *R. reptotaenium* extracts

Time	Flow (mL/min)	% Acetonitrile with 0.05% formic acid (v/v)	% Water with 0.05% formic acid (v/v)
0.00	0.30	30.0	70.0
7.00	0.30	70.0	30.0
10.00	0.30	100.0	0.0
15.00	0.30	100.0	0.0

Bacterial Community Composition of R. reptotaenium Cultures.

Individual bacterial strains were isolated from *R. reptotaenium* cultures by classic cultivation methods. 10 mg of *R. reptotaenium* biomass was streaked on 1.5% agar plates made with L1 medium. Plates were stored at 30°C for 4 days for bacterial colonies to develop. Bacterial colonies were selected based on the differences of color and morphology, and then made clonal by continuously streaking into new agar plates for four more times (Fig. 7). Single clonal bacterial colonies were selected and resuspended in 15 μl of nuclease free water in 0.2 mL PCR tubes, heated at 98^{o}C for 15 minutes, then centrifuged at 22,000 g for 3 minutes to pellet all of the cellular debris. The supernatants (13 μl) containing bacterial DNA were then transferred to new 0.2 mL tubes for PCR amplification.

Bacterial 16S rRNA genes were amplified using primers 16S rRNA forward (5’ - AGA GTT TGA TCC TGG CTC AG - 3’) and 16S rRNA reverse (5’ - ACG GCT ACC TTG TTA CGA CTT - 3'). Final PCR reaction concentrations were as follows: 5 μl of 5X PCR buffer, 1 μl

of 10 μM forward primer, 1 μl of 10 μM reverse primer, 0.25 μl polymerase, 3 μl DNA, and 14.75 μl nuclease-free water added to a final volume of 25 μl. PCR reactions were carried out with an initial denaturing step at 95^{o}C for 2 minutes, then followed by 30 cycles of 95^{o}C for 15 seconds, 68^{o}C for 15 seconds, and 72^{o}C for 45 seconds, with a final extension step at 72^{o}C for 5 minutes. The PCR products were run on an agarose gel (1% agarose, 1X Lithium Acetate Borate Buffer, 200V, 0.2 A) for 15 minutes, along with the negative control (nuclease-free water) to prior verify the qualification of PCR products. PCR products were purified using a QIAquick PCR Purification Kit (QIAGEN Inc., Valencia, CA). The 4Peaks software was used to clean up the bad signal peaks, then BLAST was used to analyze sequences in order to identify the closest relative in GenBank based on the percentage of identity and query cover (https://www.ncbi.nlm.nih.gov/blast/).

To determine the minimum medium requirements that would enable these isolated bacteria to grow, they were grown in three different types of media with six replicates per each treatment for 9 days: (1) L1, (2) L1 with 0.25% bactopeptone (HiMedia Laboratory Pvt. Ltd., Maharashtra-India), (3) L1 with 25 μM sucrose. Potential secondary metabolites of these bacteria cultures (grown in L1 with 25 μM sucrose medium) in supernatant and biomass were extracted by EtOAc and MeOH, respectively, as described above and submitted to antimalarial assays.

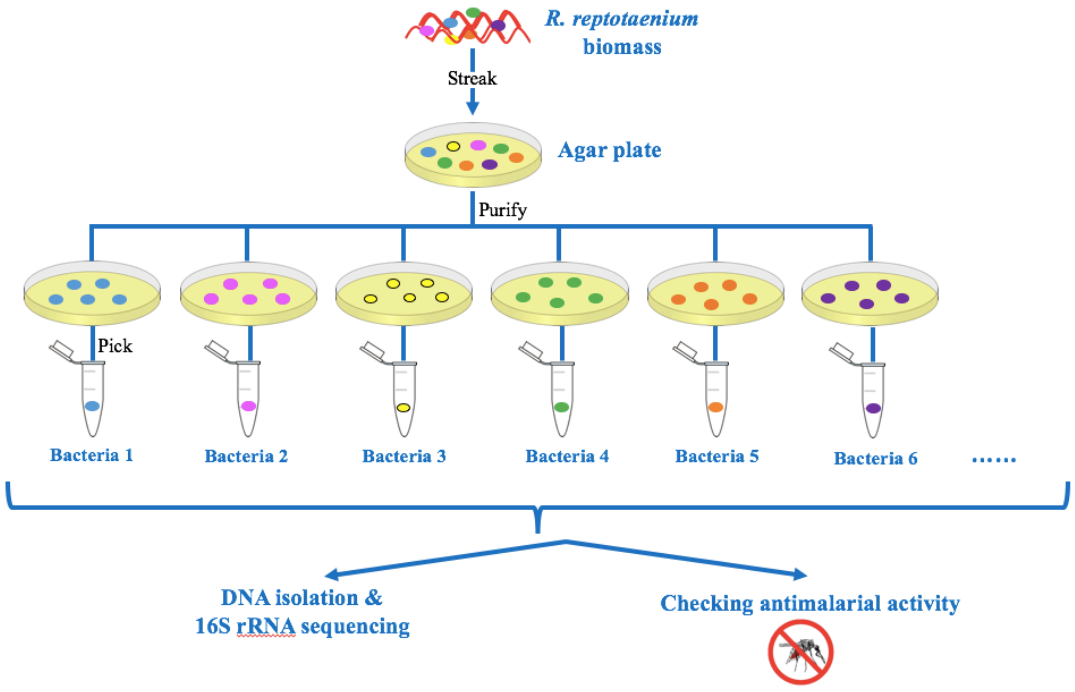

Figure 7. Protocol schematic for the identification of the roles of the bacteria community in *R. reptotaenium* culture.

Scanning electron microscopy (SEM) of *R. reptotaenium* Culture Biomass.

In scanning electron microscopy, a beam of electrons is used to image surface properties of a specimen at high resolutions unattainable by conventional light microscopy (~1 nm) (Wells 1974). Biological samples must be fixed to enable high contrast imaging.

Fixation of the samples for SEM imaging

Two and 8 weeks old suspensions of *R. reptotaenium* were fixed in 4% glutaraldehyde buffered with 0.1M sodium phosphate (pH 7.4) for 2 hours, then rinsed in the 0.1M sodium phosphate buffer for 30 min. Samples were gradually dehydrated in an ethanol series (25%, 50%, 75%, 95%) for 40 min at each gradation, followed by three 20 min washes in 100% ethanol. The cells were then processed in an automatic critical point dryer Leica Microsystems model EM

CPD300, mounted on aluminum SEM stubs, and sputter-coated with osmium. Samples were imaged using a JSM-7500F 5.0 kV SEM (JEOL USA, Inc., Peabody MA) at the Center for Advanced Microscopy in Michigan State University.

RESULTS

R. reptotaenium culturing

The original 15 mL *R. reptotaenium* culture we obtained from Bigelow laboratory contained only a small white clump of *R. reptotaenium* biomass. At the beginning, we inoculated the culture into 500 mL of L1 media and maintained it at 30°C and 27 $\mu Em^{-2}s^{-1}$ under a 12:12 light/dark cycle of cool-white light but without covering. Under these conditions, *R. reptotaenium* biomass did not increase nor was there any color change from white to red even after two months. The culture were also maintained under the light intensity equal to the intensity inside 2 layers of paper, 5 $\mu Em^{-2}s^{-1}$, which were cut off by transparency films 75% nano ceramic solar (Tint Depot, Houston, TX). However, the *R. reptotaenium* still did not increase its biomass or change its color. It was believed that the white paper may decrease the light intensity and change the light spectrum.

When we covered the flask twice by multipurpose white paper (Georgia-Pacific Consumer Products, Atlanta, GA) and maintained under the same conditions as described above, the culture increased its biomass and started to change the color from white to red after 4 weeks. We also saw that some *R. reptotaenium* filaments start to adhere onto the walls of the culture flasks, forming ring patterns approximately 3 mm in diameter. (Fig. 8).

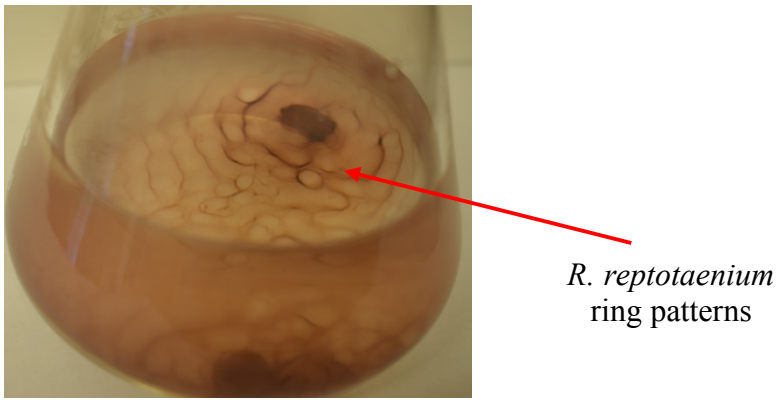

Figure 8. Ring patterns of an undisturbed 4 week-old *R. reptotaenium* culture.

Characterizing potent antimalarial/anticancer compounds in *R. reptotaenium* extracts

Antimalarial activity of R. reptotaenium crude extracts as a function of the duration of culturing.

In collaboration with Dr. Melissa Jacob's group at the National Center for Natural Products Research (NCNPR), the anti-malarial potential of bioactive metabolites derived from the *R. reptotaenium* culture was evaluated *in vitro* on a chloroquine (CQ) -sensitive strain (*P. falciparum* D6) and a CQ-resistant strain (*P. falciparum* W2). *P.falciparum* W2 (D6) IC50 is the dose that inhibits 50% growth of *P.falciparum* W2 (D6) relative to the control. Vero cells (monkey kidney cells) were used as a control to estimate general toxicity of the extracted compounds. The selective index (SI) is the ratio between the IC50 of the control (Vero) cells over the IC50 of *P. falciparum* and for promising drug lead compounds, usually falls within the range of 9-11 (M. Jacob, personal communication). The *R. reptotaenium* extracts generally showed a similar inhibition response on the *P. falciparum* D6 and W2 strains; we will show representative results using the W2 strain (Figs. 9-11) (data for the D6 strain can be found in the

appendix (Tables 7-9). Antimalarial assays were repeated twice; as the average data were very similar to the values of replicates and given only two replicates, error bars are not shown.

R. reptotaenium crude extracts were found to produce secondary metabolites with potent antimalarial activity. The antimalarial activity of *R. reptotaenium* crude extracts increased as the duration of culturing increased. For example, 8 week-old *R. reptotaenium* supernatant crude extracts inhibited 50% growth of *P.falciparum* W2 parasite with a dose of 196 ng/mL while ~15,000 ng/mL of 2 week-old *R. reptotaenium* supernatant crude extract was needed for a similar effect (Fig. 9-left). The biomass crude extracts at 8 weeks showed more potent antimalarial activity than at 2 weeks, IC50=5,500 ng/mL vs to ~17,000 ng/mL. The supernatant crude extracts were generally more potent than the biomass crude extracts at the same age. For example, the supernatant extracts at 8 weeks was 28 times more active than the biomass extracts at the same age (IC50 of 196 ng/mL compared to 5,500 ng/mL) (Fig. 9-left).

The SI value increased over time, meaning that the crude extracts of older cultures were more active than those of the younger cultures. The SI value of supernatant crude extracts increased dramatically from 3 in 2 weeks to 243 in 8 weeks (Fig.9-right). The *R. reptotaenium* culture showed the best antimalarial activity in the supernatant extracts at 8 weeks (the longest culturing time examined), with an IC50 <196 ng/mL, and an SI value of 243 (Fig.9). We speculate that if we continue maintaining the culture more than 8 weeks, the antimalarial activity will keep increasing, although we have not tried to do it yet due to the lack of culturing capacity.

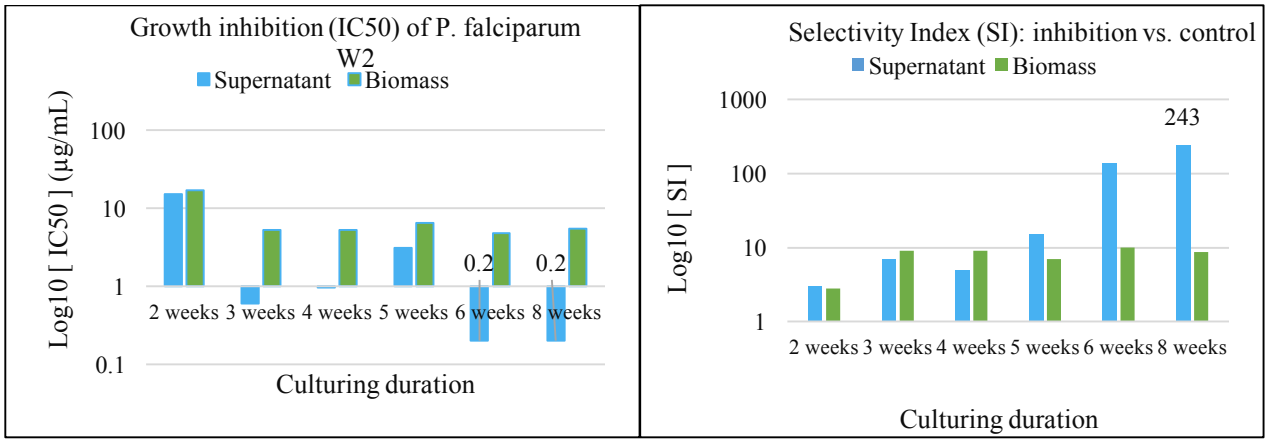

Figure 9. Growth inhibition (IC50) *P.faciparum* W2 (left) and selectivity index (SI) of inhibition vs. control (right) of *R. reptotaenium* crude extracts according to the culturing duration.

Eight week-old *R. reptotaenium* crude supernatant and biomass extracts (100 mg each) were purified through a C18 column and eluted using different concentrations of methanol (MeOH) followed by acetone. The yields for each fraction (after drying) are shown in Table 2. These eluted fractions were then submitted for antimalarial assays.

Table 2. The dry-weight yield of fractions from supernatant and biomass extracts eluted using different concentrations of methanol.

Fractions	Supernatant extracts (mg)	Biomass extracts (mg)
Water	82.54	71.88
20% MeOH	1.11	2.74
40% MeOH	0.79	1.96
60% MeOH	0.79	2.34
80% MeOH	1.27	1.18
100% MeOH	0.79	0.78
100% Acetone	0.95	1.18
Total	88.25	82.04

The water, 20% MeOH, and 40% MeOH eluted fractions from the crude supernatant crude extracts did not show any antimalarial activity. The five active fractions were 100% MeOH and 100% acetone from supernatant extracts, and the 80% MeOH, 100% MeOH, 100% acetone fractions from the crude biomass extracts. In the supernatant extracts, the 100% acetone fraction was most active, with an IC50 of 0.22 ng/mL and an SI of 216 (Fig. 10); the 100% MeOH fraction was slightly less active, with an IC50 of 1 ng/mL and an SI of 48. However, the yield of these fractions were extremely small, with only 0.95 mg of the 100% acetone fraction and 0.79mg of the 100% MeOH fraction from 100 mg of crude extracts (Table 2). The 100% acetone fraction derived from the crude supernatant extract was 27 times more potent than from the 100% acetone fraction biomass (0.22 ng/mL compared to 6 ng/mL).

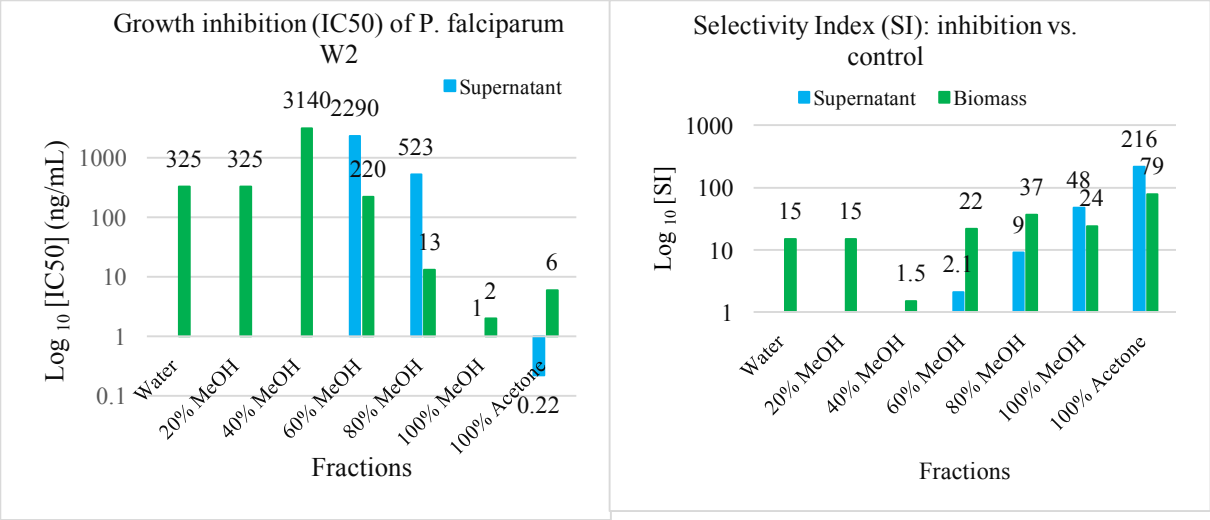

Figure 10. Growth inhibition (IC50) *P. faciparum* W2 (left) and the selectivity index (SI) of inhibition vs. control (right) of *R. reptotaenium* fractions eluted by methanol (MeOH).

Another set of 8 week-old crude supernatant and biomass extracts (100 mg per each) were loaded through a C18 column and eluted using different concentrations of acetontitrile (CH_3CN) followed by acetone. The yields of these fractions are shown in table 3. These fractions were then submitted for antimalarial assays.

Table 3. The dry-weight yield of fractions from supernatant and biomass extracts eluted using different concentrations of acetonitrile.

Fractions	Supernatant extracts (mg)	Biomass extracts (mg)
Water	91.3	91.3
20% Acetonitrile	3.1	2.5
40% Acetonitrile	0.3	0.2
60% Acetonitrile	0.3	0.3
80% Acetonitrile	0.1	0.1
100% Acetonitrile	0.3	0.1
100% Acetone	0.2	0.3
Total	95.6	94.8

The 100% acetone fractions eluted from the crude supernatant extracts were most potent, with an IC50 of 0.5 ng/mL and an SI of 1134 (Fig. 11), although the yield of this fraction (dry-weight) was low at 0.2 mg over 100 mg of input extract (Table 3). The antimalarial activity was spread out in the three last fractions (80% methanol, 100% methanol, and 100% acetone) when the crude extracts were purified by MeOH. In contrast, the antimalarial activity was focused on the last fraction (100% acetone) when the crude extracts were purified by acetonitrile.

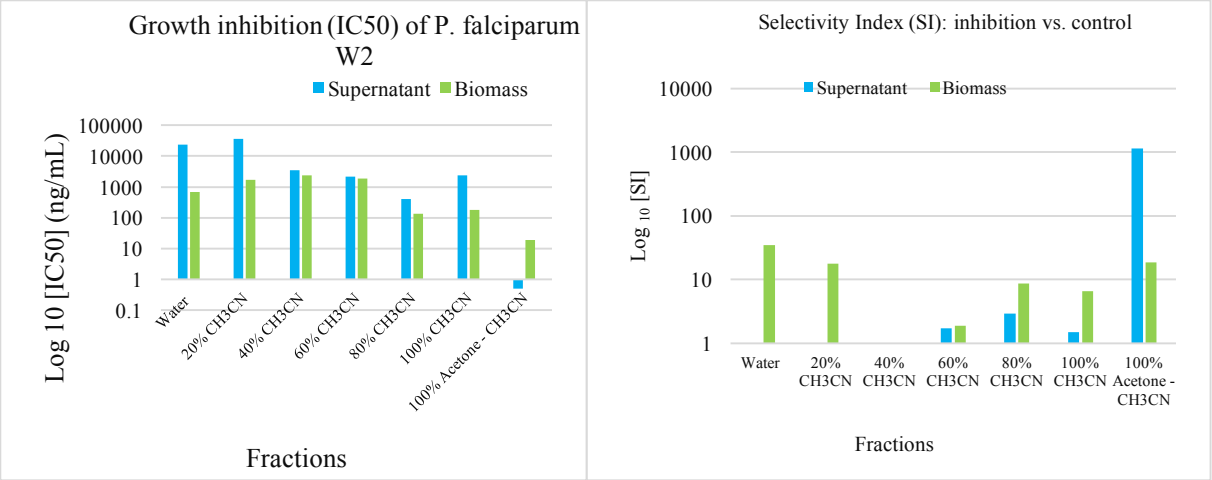

Figure 11. Growth inhibition (IC50) *P. faciparum* W2 (left) and the selectivity index (SI) of inhibition vs. control (right) of *R. reptotaenium* purified fractions by different concentrations of acetonitrile (CH_3CN).

Anticancer activity of R. reptotaenium crude extracts

In collaboration with Dr. David Pasco of the NCNPR, we determined that 8 week old *R. reptotaenium* crude extract inhibited more than 80% of Temodar drug-resistant glioblastoma brain cancer cells with an IC50 of ca. 0.1 μg/mL. However, at the same concentration, this extract only inhibited <40% of the triple-negative breast cancer cell growth. Generally, at moderate to high concentrations, the *R. reptotaenium* crude extracts were particularly effective against the Temodar drug-resistant glioblastoma cell line (Fig.12)

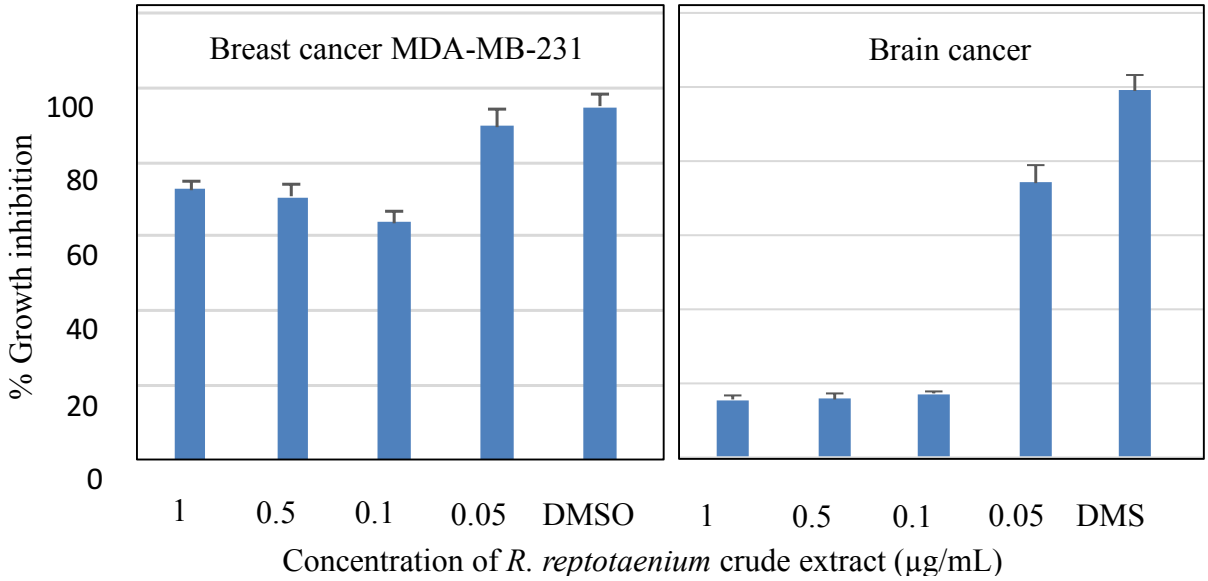

Figure 12. Anticancer activity of *R. reptotaenium* crude extracts on Temodar-resistant glioblastoma (T98G; brain cancer) and triple-negative breast cancer (MDA-MB-231) cell lines.

LC-MS of the active fractions

One gram of the 8 week-old *R. reptotaenium* crude supernatant extracts (from 40 L of culture) were fractionated using a C18 column and eluted by different concentrations of methanol and acetone as described above. The two most biologically active fractions (100% methanol and 100% acetone) were combined for a total of 13 mg (dry weight) of what we refer to as "highly active extract."

The five active fractions eluted by methanol (supernatant-100% methanol, supernatant-100% acetone, biomass-80% methanol, biomass-100% methanol, and biomass-100% acetone), two active fractions eluted by acetonitrile (supernatant-100% acetone and biomass-100% acetone), and the 13 mg of highly active extract were submitted for LC-MS analysis. All active fractions showed a similar LC elution profile within the 2-4.5 min range (Fig. 13). The 13 mg of the highly active extract was divided into 4 regional parts, and submitted for antimalarial assays.

Part 2, which contained the peaks in the 2-4.5 min region in Fig.14, was the most active part with an IC50 <4.9 ng/mL and SI of 120 (Table 4).

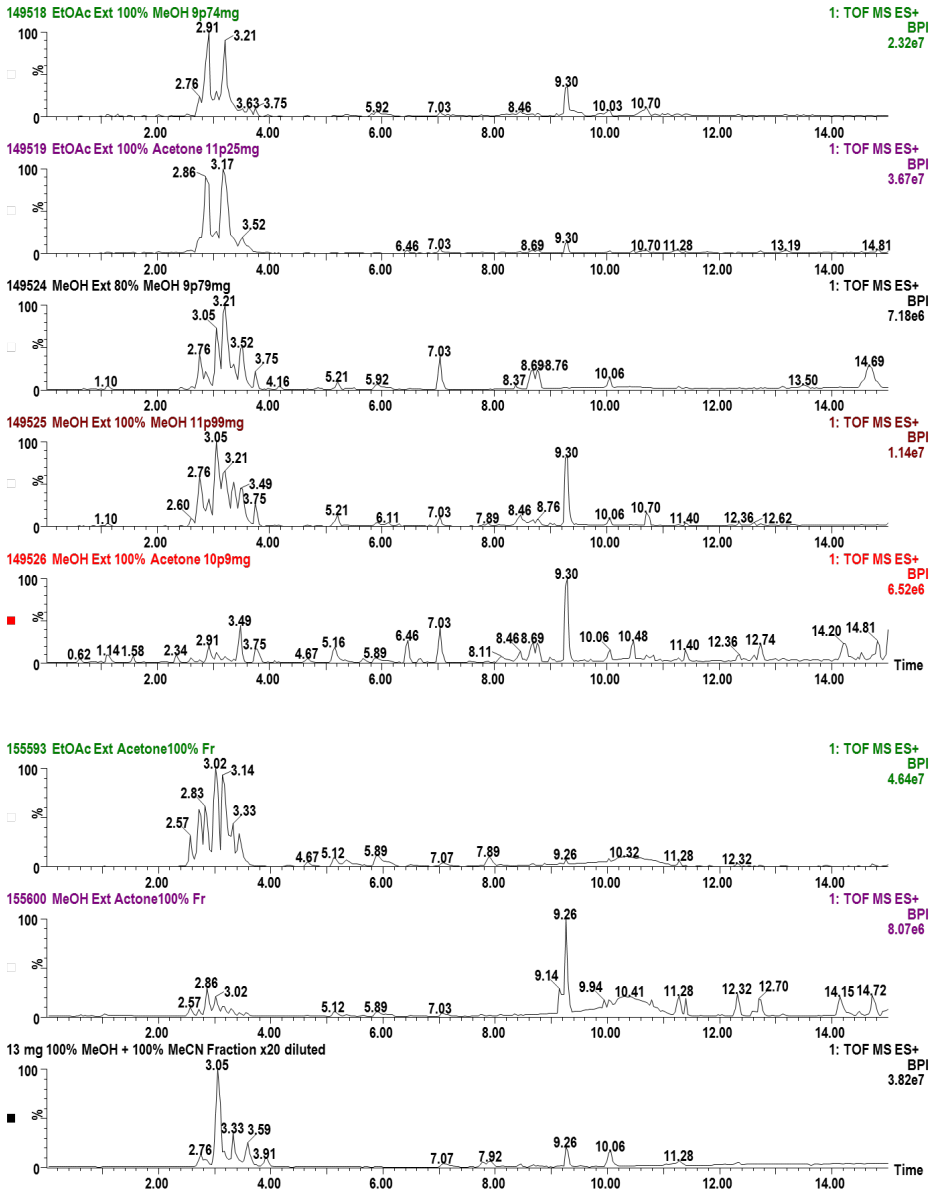

Figure 13. Liquid chromatography of the active fractions. From top to bottom: five active fractions eluted by methanol: supernatant-100% methanol, supernatant-100% acetone, biomass-80% methanol, biomass-100% methanol, and biomass-100% acetone; two active fractions eluted by acetonitrile: supernatant-100% acetone and biomass-100% acetone; 13 mg of the highly active extract (100% methanol and 100% acetone elution from the supernatant crude extract).

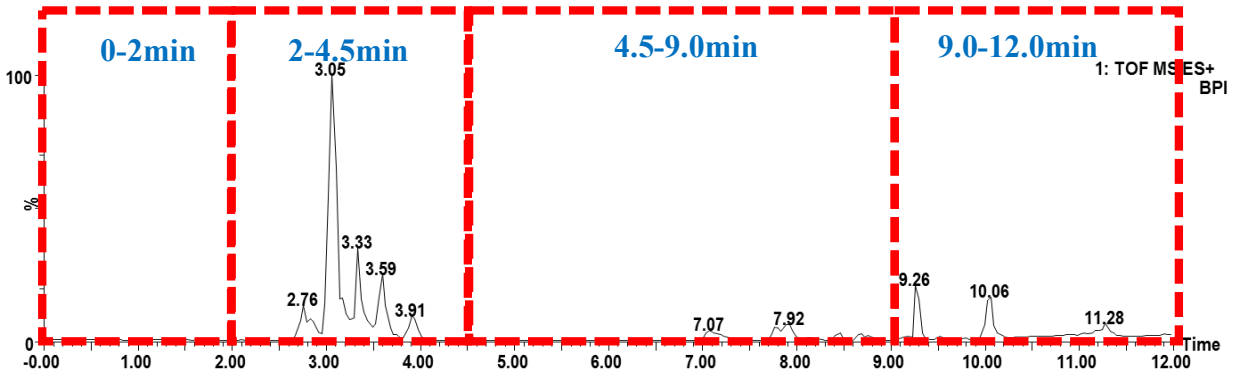

Figure 14. Liquid-chromatography of the supernatant-acetone 100% fraction.

Table 4. Antimalarial activities of different parts of an LC elution of 13 mg of the highly active extract (from 100% methanol and 100% acetone fractions of 8-week old supernatant crude extract). Part 2 contains the same peaks as those seen in Fig. 13 in the 2-4 min region.

Parts	P. falciparum W2 IC50 (ng/mL)	P. falciparum W2 SI
Part 1: 0-2.0 min	>1190	1
Part 2: 2.0-4.5 min	<4.9	120
Part 3: 4.5-9.0 min	109	>11
Part 4: 9.0-12.0 min	>1190	1
Combination	14	>86.5

Using the Table 1 LC gradient elution conditions, five compounds were repeatedly found in the active 2-4 min region (Table 5). The molecular weights of these compounds often differed by a mass of 14, which is equivalent to a methylene (CH_2) group of methylene. The MS output of two representative compounds consistently found are shown in Fig.15.

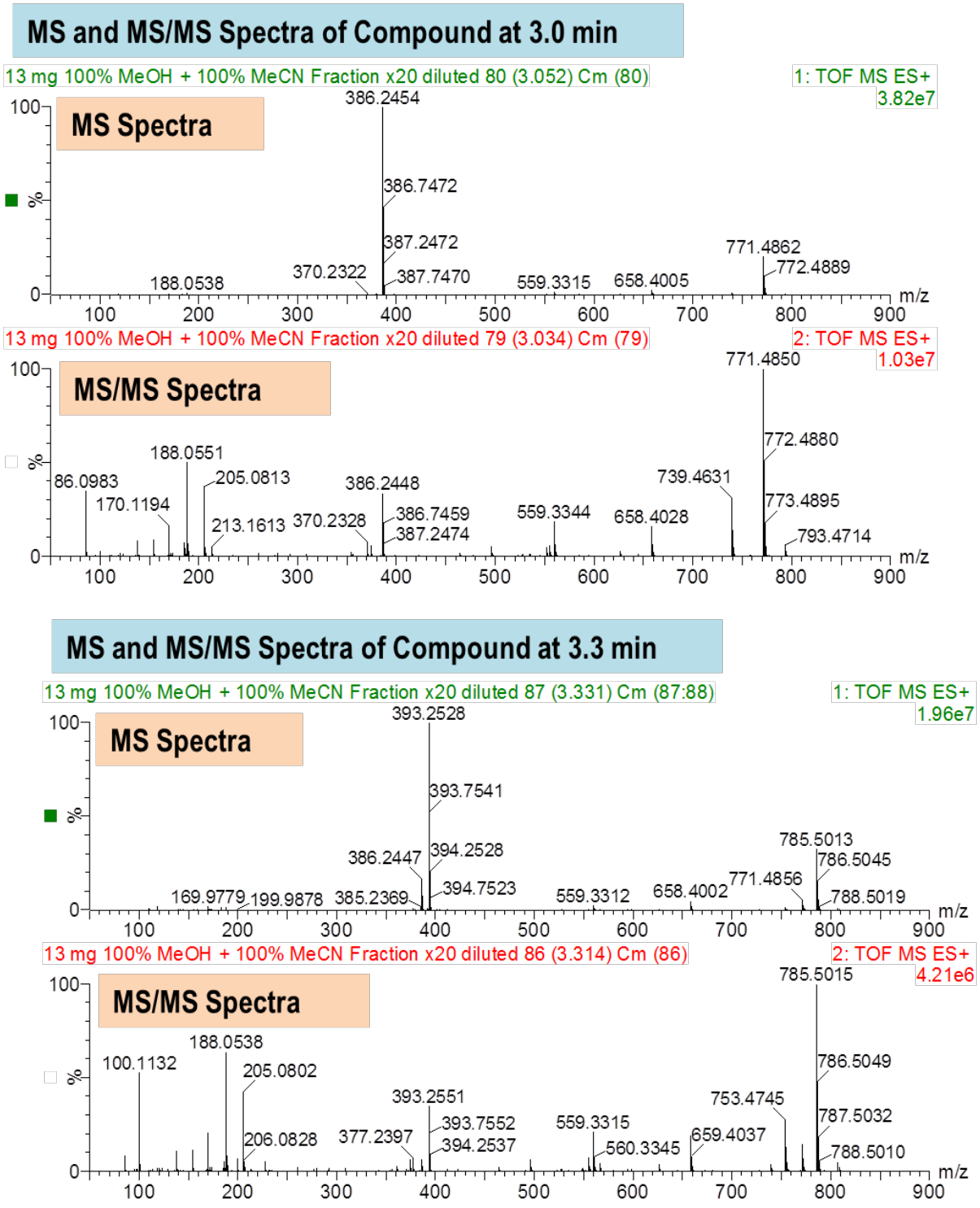

Figure 15. MS and MS/MS spectra of two representative compounds repeatedly found in the active fractions.

SciFinder (Wagner 2006) was used to search known compound databases for molecules having the same molecular weight, molecular formula, and retention times. The compound with a molecular weight of 785 was identified as likely to be dolastatin 10, a known potent anticancer and antimalarial compound (Pettit et al. 1989). The compound with a molecular weight of 770 was identified as likely to be monomethyl auristatin D (MMAD), a derivative of dolastatin 10 generated by purely synthetic means today (Miyazaki et al. 1995) (Table 6). In order to verify our assumption, pure dolastatin 10 and MMAD were obtained as the standards, and LC-MS/MS co-injection experiments with these standards and the highly active extract confirmed the identity of dolastatin 10 (Fig. 16) and MMAD in the active fractions (Fig. 17)

Table 5. The probable formula and putative compound name based on molecular weight and retention time

Retention time (min)	Molecular weight	Most probable formula	Putative compound
2.75	757	$C_{40}H_{65}N_6O_6S$	Other compound
3.05	771	$C_{41}H_{67}N_6O_6S$	Monomethyl auristatin (MMAD)
3.33	785	$C_{42}H_{69}N_6O_6S$	Dolastatin 10
3.59	801	$C_{42}H_{69}N_6O_7S$	Other compound
3.91	815	$C_{43}H_{71}N_6O_7S$	Other compound

EIC (785 Da) chromatograms of the active fraction, dolastatin 10, and mixture of dolastatin 10 plus the active fraction

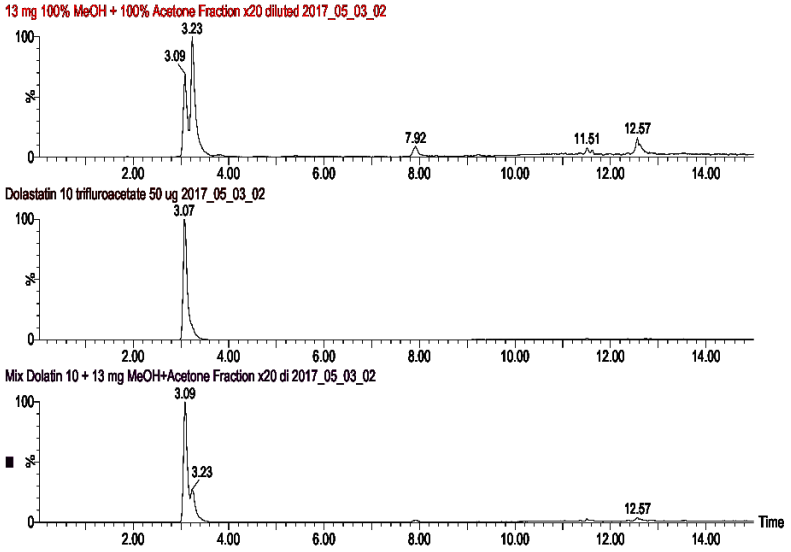

MS spectra of the active fraction, dolastatin 10, and mixture of dolastatin 10 plus the active fraction

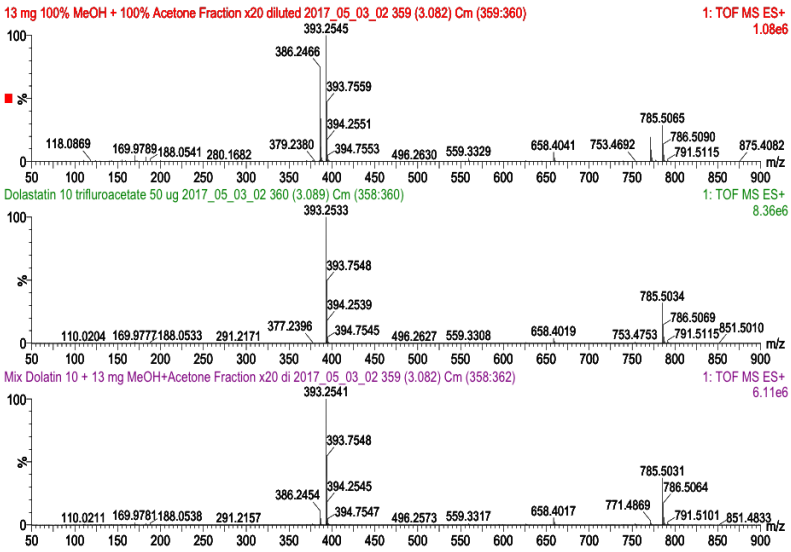

Figure 16. The chromatogram (above) and mass-spectrometry (below) of dolastatin 10 alone, dolastatin 10 co-injected with the 13 mg highly active fraction, and the 13 mg highly active fraction alone (100% methanol and 100% acetone fractions of the supernatant crude extract)

EIC (771 Da) chromatograms of the active fraction, MMAD, and mixture of MMAD plus the active fraction

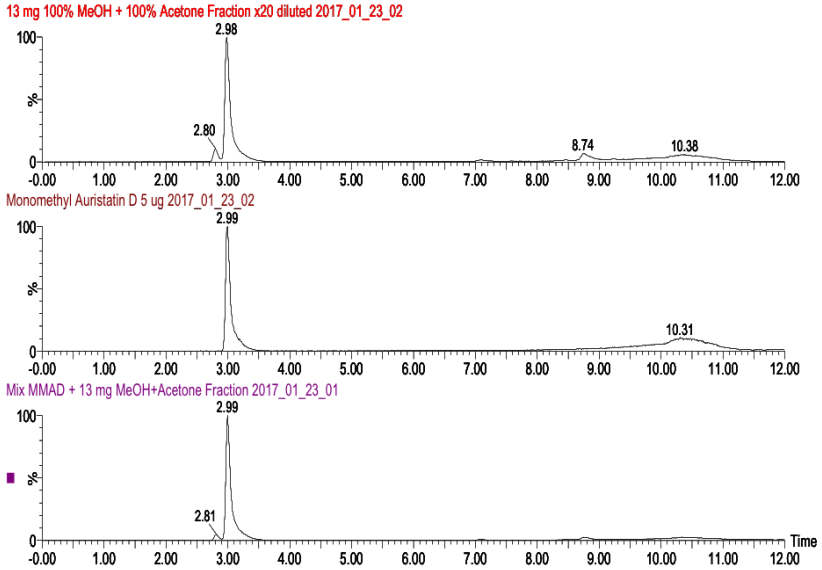

MS spectra of the active fraction, MMAD, and mixture of MMAD plus the active fraction

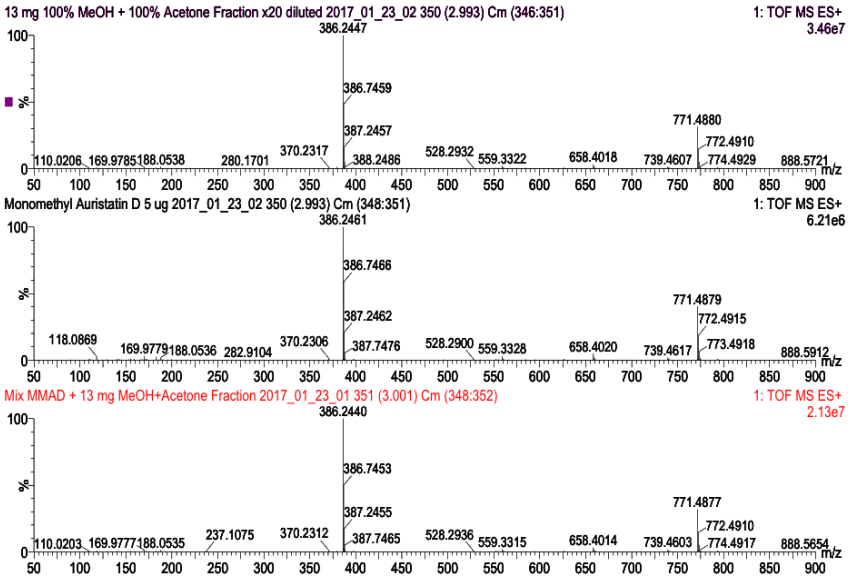

Figure 17. The chromatogram (above) and mass-spectrometry (below) of MMAD alone, MMAD co-injected with the 13 mg highly active fraction, and the 13 mg highly active fraction alone (100% methanol and 100% acetone fractions of the supernatant crude extract).

With Drs. Amar Chittiboyina and Yan-Hong Wang of the NCNPR, a possible biogenesis diagram of dominant metabolites in the active fractions was proposed (Fig. 18). The compound with molecular weight of 785 was likely dolastatin 10. The compound with molecular weight of 771 was likely MMAD. The compounds with molecular weights of 757, 801, and 815 were the other compounds (Table 5).

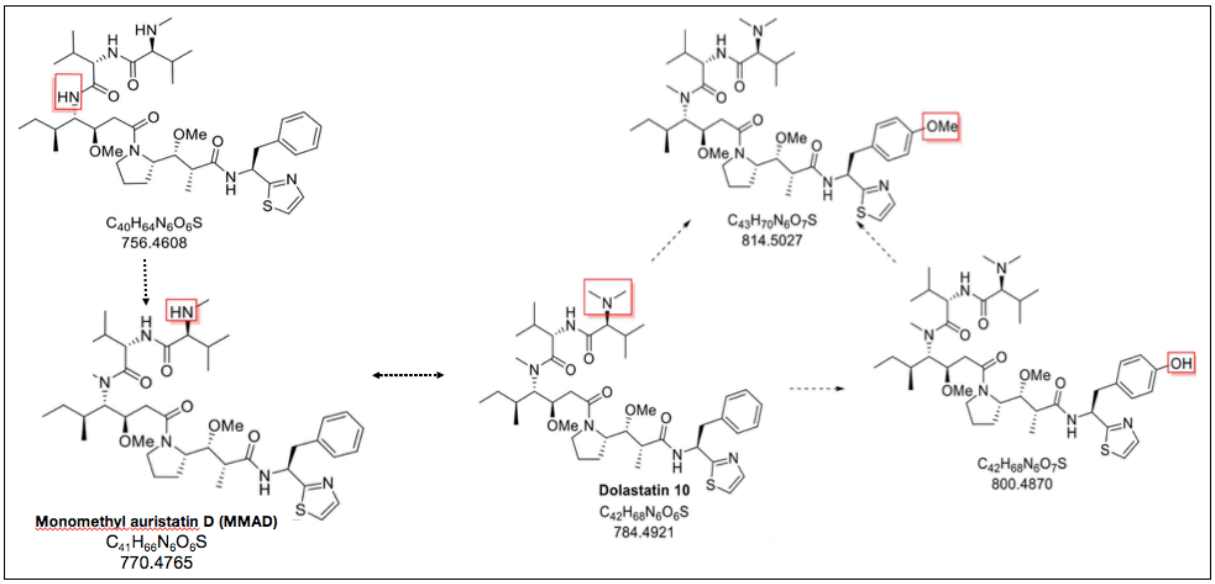

Figure 18. Proposed biogenesis of dominant metabolites in active fractions

Understanding the role of the bacteria community in *R. reptotaenium* culture.

Bacterial strains isolated from an 8 week-old R. reptotaenium culture by 16S rRNA gene amplification.

Thirty-four isolated bacterial colonies (obtained after repeated passage) were randomly selected and submitted for 16S rRNA gene amplification. The following six bacterial strains were identified: *Labrenzia (alexandrii), Labrenzia (aggregate)*, *Kordiimonas sp.*, *Muricauda sp.*, *Stappia sp.*, and *Phyllobacterium sp.* (Table 5). *Labrenzia (alexandrii)* and *Muricauda sp.* were

the two most abundant species, accounting for 29/34 colonies, while *Labrenzia alexandrii* was the least dominant species with only 6/34 colonies.

Table 6. The bacterial identity and frequency of colonies isolated from an 8 week-old *R. reptotaenium* culture (out of 34 randomly sampled colonies).

Bacterial strains	The number of colonies (out of 34 total)
Labrenzia alexandrii	2
Labrenzia aggregata	10
Kordiimonas sp.	4
Muricauda sp.	10
Stappia sp.	4
Phyllobacterium sp.	4
Total	34

Labrenzia sp., Stappia sp., Koidiimonas sp, Phyllobacterium sp. belong to α-Proteobacteria while *Muricauda sp.* are in the Flavobacteria phylum. All of these bacterial strains are marine heterotrophic, gram-negative bacteria. Their sizes range from 0.1 to 3.0 μm, and are generally rod-shaped. More detailed information of the six bacterial strains can be found in the Appendix (Table 10).

Growing bacterial strains in different types of media and biological activity of extracts

The six different culturable bacteria isolated from the *R. reptaenium* polyculture were grown in three different types of media over a 9 day-period to determine the minimum medium in which these species could grow. The L1 media was the negative control while the L1 with

peptone media was the positive control. The heterotrophic bacteria did not grow in L1 media due to a lack of a carbon source. Fig. 19 showed that L1 containing sucrose [0.25 μM] was the minimum medium in which the six bacterial strains could grow after 9 days.

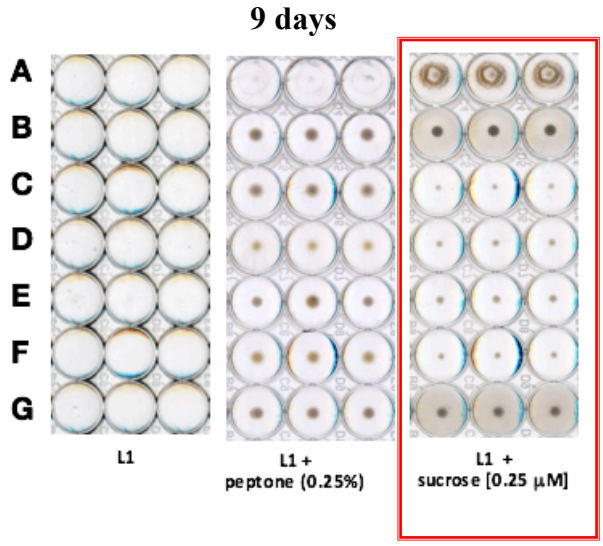

Figure 19. Species isolated and identified by 16S gene sequencing from *the R. reptotaenium* polyculture (A. *Labrenzia alexandrii*, B. *Labrenzia aggregata*, C. *Kordiimonas* sp., D. *Muricauda* sp., E. *Stappia* sp. F. *Phyllobacterium* sp. G. 6 of the bacteria (A-F) growing together) were grown in 6 different types of media during 9 days.

The supernatant and biomass extracts of the bacteria growing alone and 6 bacteria growing together (grown in L1 containing sucrose) did not show any antimalarial activity. The IC50 concentration of almost all the bacterial strains (except *L. alexandrii*) was >47600 ng/mL and the SI was 1. The IC50 of *L. alexandrii* supernatant extracts was >28000 ng/mL, and the SI was <1.7 (Table 11-appendix B).

SEM images

SEM of 8 week-old *R. reptotaenium* culture biomass showed several bacteria attached to the cell walls of the filamentous *R. reptotaenium* (Fig. 20a). These bacteria exhibit various morphologies and sizes (Fig. 20b). At least one bacterial strain secretes extracellular polysaccharide webby projections into *R. reptotaenium* cells (Fig. 20c&d). These webby projections may explain in part why all former attempts to isolate axenic *R. reptotaenium* cultures have been unsuccessful. Strong antibiotic treatments and physical attempts (micropipette isolation) to separate the cell-wall-associated bacteria may significantly damage the cyanobacterial cells (Casamatta et al. 2012).

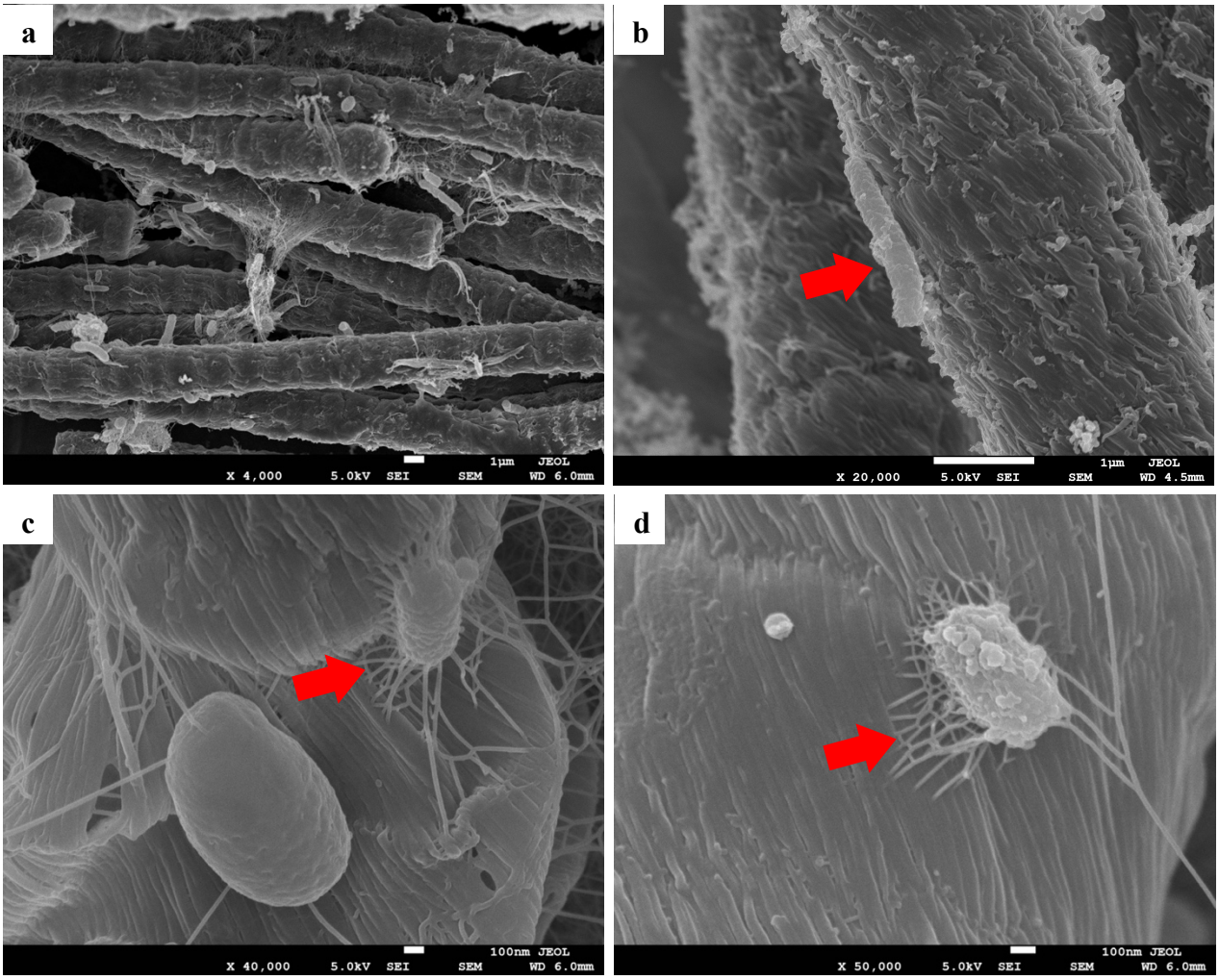

Figure 20. SEM images of biomass samples of 8 week-old *R. reptotaenium* culture. (a) *R. reptotaenium* filaments with several associated bacteria on their cell walls (4,000X); (b) bacterium (red arrow) attached on *R. reptotaenium* filament (20,000X); (c, d) bacteria attached to *R. reptotaenium* filaments via extracellular polysaccharide webby projections (red arrows) (40,000X and 50,000X).

Metagenomics (16S) amplicon sequencing results showed that in addition to Cyanobacteria, there are dominant bacteria in the culture from the phyla of Bacteroidetes,

Planctomycetes, and Proteobacteria, with 50% of the community composition being from the (α-Proteobacteria subphylum (Fig. 21).

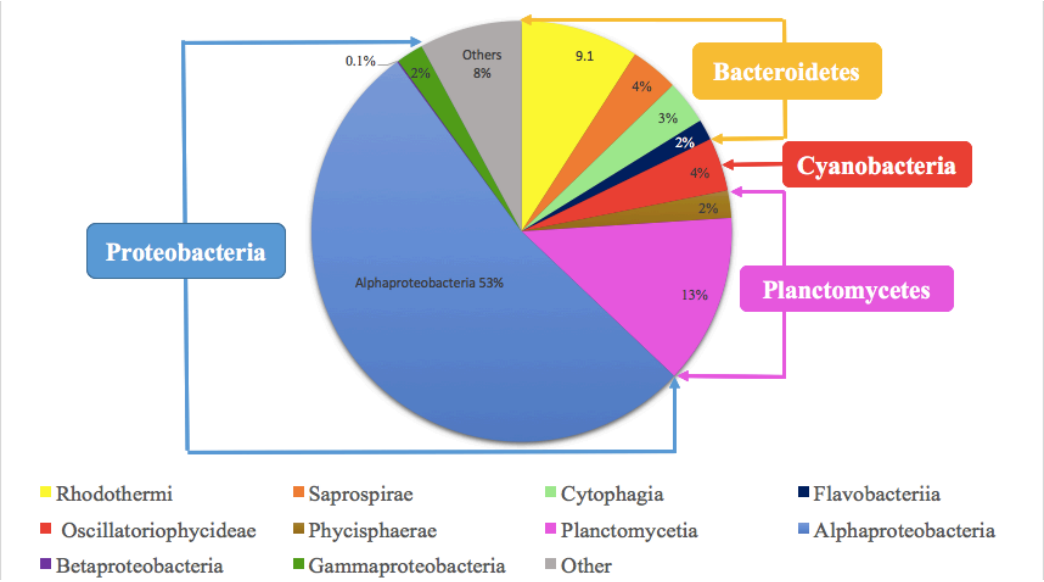

Figure 21. The relative abundance of four most dominant bacterial phyla in *R. reptotaenium* 8 weeks-old culture.

DISCUSSION

The antimalarial activity of *R. reptotaenium* extracts

Overall, the *R. reptotaenium* supernatant extracts showed more potent antimalarial activity than the biomass extracts. For example, the antimalarial activity of the 8 week-old supernatant crude extracts was 28 times more potent than the biomass crude extracts of the same age (IC50 196 ng/ml to IC50 5500 ng/mL) (Fig. 8). In addition, the supernatant-100% acetone fraction eluted by methanol was 27 times more active than the biomass-100% acetone fraction eluted by the same solvent (IC50 0.22ng/mL to a ratio of IC50 6 ng/mL) (Fig. 9). The supernatant-100% acetone fraction eluted by acetonitrile was 38 times more active than the biomass-100% acetone fraction eluted by the same solvent (IC50 0.5ng/mL to a ratio of IC50 19 ng/mL) (Fig. 10). It is not readily apparent why the antimalarial activity of the supernatants always outperformed the biomass in the antimalarial assays. We speculate that the underlying reason is possibly due to dolastatin 10 and MMAD being extracellular compounds, not intracellular compounds, meaning that *R. reptotaenium* polycultures can readily excrete these compounds into their environment. This may also explain why former attempts to isolate dolastatin 10 from the biomass of sea hare *Dolabella auricularia* (Pettit et al. 1987, 1993) and the biomass of the marine cyanobacteria *Symploca* sp. VP642 (Luesch et al. 2001) produced substantially smaller yields, at 10^{-7} % and ~10^{-2} % dry weight yields, respectively (Pettit et al. 1987, 1993, Luesch et al. 2001). These extremely small yields contributed to the 15 year process of completely elucidating the chemical structure of dolastatin 10. Dolastatin 10 and MMAD are

two well-known microtubule inhibitors, that can act against various cancer cells with picomolar concentration.

The 100% acetone fraction eluted by MeOH and the 100% acetone fraction eluted by acetonitrile (CH_3CN) were more active than antimalarial drugs currently on the market. The 100% acetone fraction eluted by methanol was the most active fraction, inhibiting 50% growth of *P. falciparum* parasites at a concentration of 0.22 ng/mL, in contrast to 5.37 ng/mL of Artemisinin or 7.92 ng/mL of Chloroquine (Fig.22- left). The 100% acetone fraction eluted by acetonitrile had the highest SI value at 1134 (Fig. 22- right).

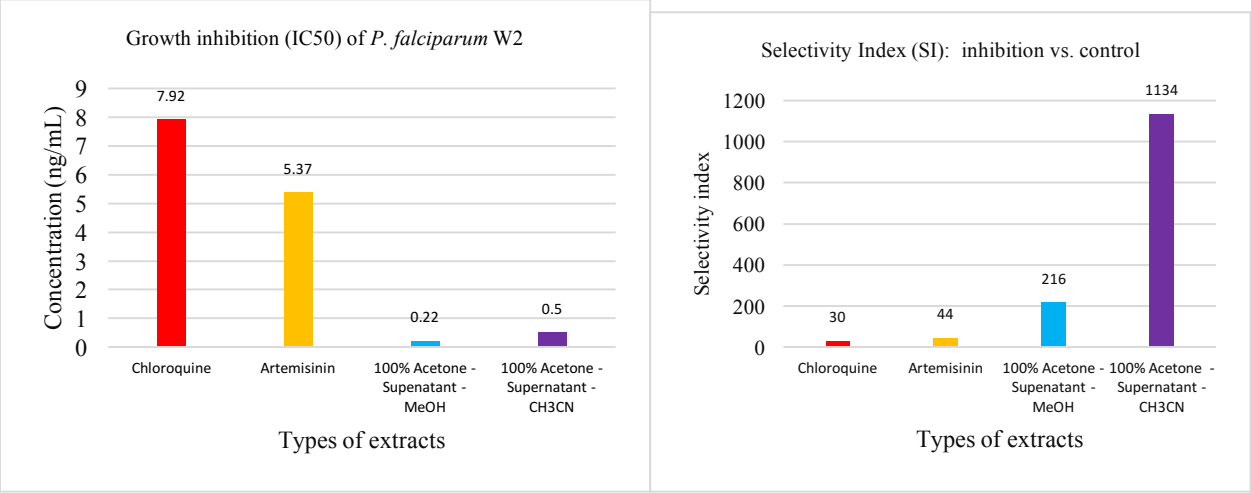

Figure 22. Growth inhibition (IC50) *P. faciparum* W2 (left) and Selective specificity of inhibition vs. control (right) of *R. reptotaenium* extracts compared to the current antimalarial medicines on the market.

The role of culture duration and the *R. reptotaenium* associated bacterial community in producing dolastatin 10

In the process of isolating and culturing the bacteria associated with *R. reptotaenium* cultures, the colonies with distinctive colors and morphologies were sequenced by 16S rRNA gene amplification and identified as six different bacterial strains (Table 6). Five of the six

bacteria identified through this method belonged to the α-Proteobacteria subphylum, with the sixth bacterial strain belonging to the Flavobacteria subphylum (Table 6). This single colony sequencing data was generally similar to the whole genome metagenomic sequencing data, in which the α-Proteobacteria subphylum accounted for 53%, while the Flavobacteria subphylum accounted 2% relative abundance over the whole community (Fig. 20). However, no bacterial strains in Bacteroidetes and Planctomycetes were found by using the single colony sequencing method, although these phyla accounted for a large percentage of relative abundance, 13.2% and 12.7%, respectively, in the whole genome metagenomic sequencing data (Fig. 20). Unfortunately, the SEM images could not be used alone to identify the bacterial strains, although parallel in-situ FISH probes targeting species-specific gene sequences might be able to be used with TEM for accurate bacterial strain identification. The secondary metabolites of the heterotrophic bacteria isolated from *R. reptotaenium* cultures did not show antimalarial activity. More bacterial isolation should be done to verify whether the bacterial strains in these subphyla were unculturable or not yet identified, and whether they show any bioactivity. The roles that the bacterial strains played in producing the suit of dolastatin-like complex of compounds were inconclusive. However, we have shown strong evidence that dolastatin 10 and its synthetic analogue MMAD are produced through a novel source, the marine cyanobacteria *R. reptotaenium*. At this point, we speculate that the bacteria could be adding a methylene group (CH_2) into MMAD to produce dolastatin 10, or be removing a CH_2 group from dolastatin 10 to generate MMAD (Fig. 23).

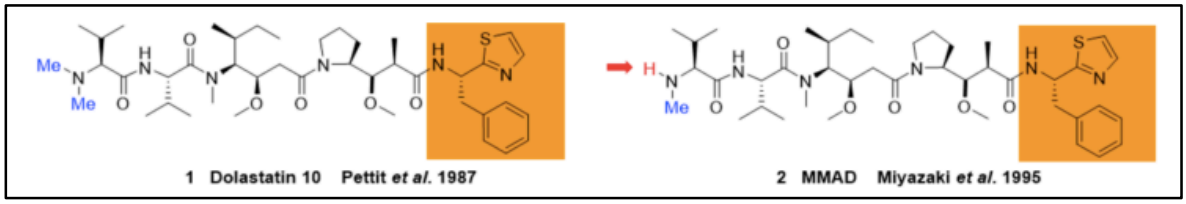

Figure 23. Monomethyl auristatin D (MMAD) was modified from dolastatin 10

Other analogues of dolastatin 10 (Lyngbyastatin 1 and 4, dolastatin 12 and 13) were isolated from the marine cyanobacteria *Lyngbya* sp. (Harrigan et al. 1998; Matthew et al. 2007). Not surprisingly, *R. reptotaenium* belongs to the same *Oscillatoriales* order as *Symploca* sp., and *Lyngbya* sp. The *Lyngbya* sp. and *Symploca* sp. samples used to extract dolastatin 10 and its analogues were collected from the field, therefore, it is likely that these cyanobacteria were also impure, with some marine bacteria living in association with the cyanobacteria. *R. reptotaenium* comprised the polyculture in the current study, while also containing some heterotrophic bacteria living in association with the cyanobacteria. Presently, it is still unknown if dolastatin 10 is synthesized by only the cyanobacteria or by the interaction between the cyanobacteria and its associated bacteria. It is evident however that dolastatin 10 and MMAD increased in concentration as the *R. reptotaenium* cultures aged. We are unsure of whether the compounds simply accumulate over time, or whether the bacterial community shifted, causing more compounds to be synthesized. Evidently more research is needed to better understand the chemical ecology and genetic basis by which dolastatin 10 and MMAD compounds are produced in the context of this microbial community.

R. reptotaenium and Black Band Disease

According to Richardson's hypothesis (2014), BBD was caused by the synergistic impacts of microcystin-LR toxin produced by *R. reptotaenium* and sulfide produced by sulfate

reducing bacteria (Richardson et al. 2014). *R. reptotaenium* could produce microcystin-LR with a concentration of 0.02 - 0.04 mg g^{-1} determined by using the enzyme-linked immunosorbent assay (ELISA) test (Stanić et al. 2011). However, in the process of isolating dolastatin 10 and MMAD from *R. reptotaenium* polycultures, we did not see any compound with a molecular weight of 995 - microcystin LR. The Richardson group did use the high-performance liquid chromatography (HPLC) to isolate the microcystin-LR peak and compared it to the standard. However, the microcystin-LR yield was reported based on the results of an ELISA test. We still do not know whether the *R. reptotaenium* polycultures shift compositionally over time, and cease production of MC-LR, or as in the case of Richardson (2014) whether the antibodies in the ELISA test kit simply showed cross-reactivity with compounds other than microcystin-LR. It is still inconclusive as to whether microcystin-LR is the main cause of BBD or whether the cytotoxicity of the suit of dolastatin-like complex of compounds induces coral fatality. Lastly, the potential for the dolastatin-like complex to induce Black Band Disease in corals should be also carefully studied, given the destructiveness of this disease on corals worldwide.

What is dolastatin 10 and MMAD?

Dolastatin 10 and MMAD are two well-known microtubule inhibitors with important medical applications. Dolastatin 10 can act against various cancer cells by inhibiting microtubule assembly, then inducing cell cycle arrest and apoptosis. Dolastatin 10 has also shown potent antimalarial activity by inhibiting 50% of *P.falciparum* with only 10^{-10} M (Fennell et al. 2003). Despite the promising preclinical data, the phase II trial of dolastatin 10 was not successful and further clinical trials of dolastatin 10 are not recommended, due to its significant toxicity at the maximum tolerated dose (von Mehren et al. 2004; Perez et al. 2005). MMAD had a clinical application as a playload in antibody-drug conjugates (ADCs) (Senter and Sievers 2012) despite

slightly less potency than dolastatin 10 (Miyazaki et al. 1995). ADCs, an important class of potent biopharmaceutical drugs, are designed to kill only cancer cells and leave healthy cells undamaged (Bakhtiar 2016). ADCs contain 3 parts: a monoclonal antibody, a linker, and a playload (a cytotoxic anticancer compound) (Zolot, Basu, and Million 2013). MMAD can be attached to a linker and subsequently conjugated to monoclonal antibodies because it has a secondary amine at the N-terminus, a chemical characteristic dolastatins 10 do not have (Maderna et al. 2014; Senter and Sievers 2012). After being released into the cancer cells, MMAD will inhibit microtubule assembly, subsequently inducing cell apoptosis.

Dolastatin 10 and MMAD are still very expensive on the current pharmaceutical market. Respectively, dolastatin 10 and MMAD cost approximately $900 and $500 per mg. Further research can potentially focus on producing *R. reptotaenium* cultures able to synthesize dolastatin 10 and MMAD in a shorter amount of time. Such research may lead to increased yields of dolastatin 10 and MMAD. Finally, more experiments should be conducted to determine the genetic or biological pathways of dolastatin 10 and the dolastatin-like complex of compounds. Once such principles are uncovered, dolastatin may be produced on an industrial scale at a far cheaper market price by cloning the gene into *E-coli*.

LIST OF REFERENCES

Antonius, A. 1977. “Coral Mortality in Reefs: A Problem for Science and Management.” In *Third International Coral Reef Symposium*, , 617–23.

Bakhtiar, Ray. 2016. “Antibody Drug Conjugates.” *Biotechnology Letters* 38(10): 1655–64.

Buerger, Patrick et al. 2016. “Genetic , Morphological and Growth Characterisation of a New Roseofilum Strain (Oscillatoriales , Cyanobacteria) Associated with Coral Black Band Disease.” *PeerJ* 4: e2110.

Casamatta, Dale, Dina Stanić, Miroslav Gantar, and Laurie L. Richardson. 2012. “Characterization of Roseofilum Reptotaenium (Oscillatoriales, Cyanobacteria) Gen. et Sp. Nov. Isolated from Caribbean Black Band Disease.” *Phycologia* 51(5): 489–99.

Castenholz, Richard W. 1988. “Culturing Methods for Cyanobacteria.” *Methods in enzymology* 167: 68–93.

Cesar, Herman S J. 2002. “Coral Reefs: Their Functions, Threats and Economic Value.” *OceanDocs* 1: 14–39.

Correa, A. M S et al. 2009. “Symbiodinium Associations with Diseased and Healthy Scleractinian Corals.” *Coral Reefs* 28(2): 437–48.

Crossland, C. J., B.G. Hatcher, and S.V.Smith. 1991. “Role of Coral Reefs in Global Ocean Production.” *Coral Reefs* 10(2): 55–64.

Daily, Abigail, Noel R. Monks, Markos Leggas, and Jeffrey A. Moscow. 2010. “Abrogation of Microcystin Cytotoxicity by MAP Kinase Inhibitors and N-Acetyl Cysteine Is Confounded by OATPIB1 Uptake Activity Inhibition.” *Toxicon* 55(4): 827–37. http://dx.doi.org/10.1016/j.toxicon.2009.11.019.

Dass, CHHABIL. 2007. “Fundamentals of Contemporary Mass Spectrometry.” *Nature*

Biotechnology 1: 151–194.

Falconer, I R, R B Jackson, B J Langley, and M T Runnegar. 1981. "Liver Pathology in Mice in Poisoning by the Blue-Green Alga Microcystis Aeruginosa." *Australian Journal of Biological Sciences* 34(2): 179–88.

Fennell, B. J., S. Carolan, G. R. Pettit, and A. Bell. 2003. "Effects of the Antimitotic Natural Product Dolastatin 10, and Related Peptides, on the Human Malarial Parasite Plasmodium Falciparum." *Journal of Antimicrobial Chemotherapy* 51(4): 833–41.

Garzón-Ferreira, J., D. L. Gil-Agudelo, L. M. Barrios, and S. Zea. 2001. "Stony Coral Diseases Observed in Southwestern Caribbean Reefs." *Hydrobiologia* 460: 65–69.

Harborne, Alastair R. et al. 2006. "The Functional Value of Caribbean Coral Reef, Seagrass and Mangrove Habitats to Ecosystem Processes." *Advances in Marine Biology* 50(5): 57–189.

Harrigan, George G. et al. 1998. "Isolation, Structure Determination, and Biological Activity of Dolastatin 12 and Lyngbyastatin 1 from Lyngbya majuscula/Schizothrix Calcicola Cyanobacterial Assemblages." *Journal of Natural Products* 61(10): 1221–25.

Harvell, Drew et al. 2001. "Coral Bleaching and Disease: Contributors to 1998 Mass Mortality in Briareum Asbestinum (Octocorallia, Gorgonacea)." *Hydrobiologia* 460: 97–104.

Hooser, S B. 2000. "Fulminant Hepatocyte Apoptosis in Vivo Following Microcystin-LR Administration to Rats." *Toxicologic pathology* 28(5): 726–33. http://www.ncbi.nlm.nih.gov/pubmed/11026609.

Jackson, Colin R, Bram W G Stone, and Heather L Tyler. 2015. "Emerging Perspectives on the Natural Microbiome of Fresh Produce Vegetables." *Agriculture* 5(2): 170–87.

Kirk, Nathan L, Jessica R. Ward, and Mary Alice Coffroth. 2005. "Stable *Symbiodinium* Composition in the Sea Fan *Gorgonia Ventalina* during Temperature and Disease Stress."

The Biological Bulletin 209(3): 227–34. http://www.ncbi.nlm.nih.gov/pubmed/16382170.

König, Jörg, Annick Seithel, Ulrike Gradhand, and Martin F. Fromm. 2006. "Pharmacogenomics of Human OATP Transporters." *Naunyn-Schmiedeberg's Archives of Pharmacology* 372(6): 432–43.

Lesser, Michael P. et al. 2007. "Are Infectious Diseases Really Killing Corals? Alternative Interpretations of the Experimental and Ecological Data." *Journal of Experimental Marine Biology and Ecology* 346: 36–44.

Luesch, H. et al. 2001. "Isolation of Dolastatin 10 from the Marine Cyanobacterium Symploca Species VP642 and Total Stereochemistry and Biological Evaluation of Its Analogue Symplostatin 1." *Journal of Natural Products* 64(7): 907–10.

Luesch, H, G G Harrigan, G Goetz, and F D Horgen. 2002. "The Cyanobacterial Origin of Potent Anticancer Agents Originally Isolated from Sea Hares." *Current medicinal chemistry* 9(20): 1791–1806. http://www.ncbi.nlm.nih.gov/pubmed/12369878.

MacKintosh, Carol, Beattie, Kenneth, Klumpp, Susanne, Schluter, Philip J, and Geoffrey A Codd. 1990. "Cyanobacterial Microcystin-LR Is a Potent and Specific Inhibitor of Protein Phosphatases 1 and 2A from Both Mammals and Higher Plants." *Federarion of European Biochemical Societies* 264(2): 187–92.

Maderna, Andreas et al. 2014. "Discovery of Cytotoxic Dolastatin 10 Analogues with N‑Terminal Modifications." *Journal of Medicinal Chemistry* 10(57): 10527–43.

Mantoura, R F C, and C A Llewellyn. 1983. "The Rapid Determination of Algal Chlorophyll and Carotenoid Pigments and Their Breakdown Products in Natural Waters by Reverse-Phase High-Performance Liquid Chromatography." *Analytica Chimica Acta* 151: 297–314.

Matthew, Susan et al. 2007. "Lyngbyastatin 4, a Dolastatin 13 Analogue with Elastase and

Chymotrypsin Inhibitory Activity from the Marine Cyanobacterium Lyngbya Confervoides." *Journal of Natural Products* 70(1): 124–27.

von Mehren, M et al. 2004. "Phase II Trial of Dolastatin-10, a Novel Anti-Tubulin Agent, in Metastatic Soft Tissue Sarcomas." *Sarcoma* 8(4): 107–11.

Miyazaki, Koichi et al. 1995. "Synthesis and Antitumor Activity of Novel Dolastatin 10 Analogs." *Chemical and Pharmaceutical Bulletin* 43(10): 1706–18.

Monk, Noel R., Shuqian Liu, and Jeffrey A Moscow. 2015. "Microcystins as Agents for Treatment of Cancer." *Pharmaceutical Sciences Faculty Patent*: 35.

Monks, Noel R et al. 2007. "Potent Cytotoxicity of the Phosphatase Inhibitor Microcystin LR and Microcystin Analogues in OATP1B1- and OATP1B3-Expressing HeLa Cells." *Molecular cancer therapeutics* 6(2): 587–98. http://www.ncbi.nlm.nih.gov/pubmed/17308056.

Niedermeyer, Timo, and Mark Brönstrup. 2012. "Natural-Product Drug Discovery from Microalgae." *Microalgal Biotechnology: Integration and Economy*: 169–200.

Perez, Edith A et al. 2005. "Phase II Trial of Dolastatin-10 in Patients with Advanced Breast Cancer." *Investigational New Drugs* 23: 257–61.

Peters, Esther C. 1984. "A Survey of Cellular Reactions to Environmental Stress and Disease in Caribbean Scleractinian Corals." *Helgolander Meeresuntersuchungen* 37(1–4): 113–37.

Pettit, George R et al. 1987. "The Isolation and Structure of a Remarkable Marine Animal Antineoplastic Constituent: Dolastatin 10." *Journal of the American Chemical Society* 109(22): 6883–85.

Pettit, George R. et al. 1989. "The Absolute Configuration and Synthesis of Natural (-)-Dolastatin 10." *Journal of the American Chemical Society* 111(14): 5463–65.

http://dx.doi.org/10.1021/ja00196a061.

———. 1993. “Isolation of Dolastatins 10-15 from the Marine Mollusc Dolabella Auricularia.” *Tetrahedron* 49(41): 9151–70.

Pitt, James J. 2009. “Principles and Applications of Liquid Chromatography-Mass Spectrometry in Clinical Biochemistry.” *The Clinical Biochemist Reviews* 30(1): 19–34.

Pochon, Xavier, Juan I Montoya-Burgos, Benoit Stadelmann, and Jan Pawlowski. 2006. “Molecular Phylogeny, Evolutionary Rates, and Divergence Timing of the Symbiotic Dinoflagellate Genus Symbiodinium.” *Molecular phylogenetics and evolution* 38(1): 20–30.

Rasoulouniriana, Diana et al. 2009. “Pseudoscillatoria Coralii Gen . Nov ., Sp . Nov ., a Cyanobacterium Associated with Coral Black Band Disease (BBD).” *Diseases of Aquatic Organisms* 87: 91–96.

Richardson, Laurie L, Miller, Aaron W, and Longin Broderick, Emily, Kaczmarsky. 2009. “Sulfide, Microcystin, and the Etiology of Black Band Disease.” *Diseases of Aquatic Organisms* 87(Richardson 2004): 79–90.

Richardson, Laurie et al. 2014. “Ecology and Physiology of the Pathogenic Cyanobacterium Roseofilum Reptotaenium.” *Life* 4(4): 968–87. http://www.mdpi.com/2075-1729/4/4/968/.

Richardson, Laurie L. 1998. “Coral Diseases: What Is Really Known?” *Trends in Ecology and Evolution* 13(11): 438–43.

Richardson, Laurie L., and Kevin G. Kuta. 2003. “Ecological Physiology of the Black Band Disease Cyanobacterium Phormidium Corallyticum.” *FEMS Microbiology Ecology* 43(3): 287–98.

Sainis, Ioannis et al. 2010. “Cyanobacterial Cyclopeptides as Lead Compounds to Novel Targeted Cancer Drugs.” *Marine Drugs* 8(3): 629–57.

Santavy, D L et al. 2001. “Quantitative Assessment of Coral Diseases in the Florida Keys : Strategy and Methodology.” *Hydrobiologia* 460: 39–52.

Schloss, Patrick D et al. 2009. “Introducing Mothur: Open-Source, Platform-Independent, Community-Supported Software for Describing and Comparing Microbial Communities.” *Applied and environmental microbiology* 75(23): 7537–41.

Schloss, Patrick D, Dirk Gevers, and Sarah L Westcott. 2011. “Reducing the Effects of PCR Amplification and Sequencing Artifacts on 16S rRNA-Based Studies.” *PloS one* 6(12): e27310.

Senter, Peter D, and Eric L Sievers. 2012. “The Discovery and Development of Brentuximab Vedotin for Use in Relapsed Hodgkin Lymphoma and Systemic Anaplastic Large Cell Lymphoma.” *Nature Biotechnology* 30(7): 631–37.

Sheng, Jian W., Miao He, and Han Chang Shi. 2007. “A Highly Specific Immunoassay for Microcystin-LR Detection Based on a Monoclonal Antibody.” *Analytica Chimica Acta* 603(1): 111–18.

Stanić, Dina, Stuart Oehrle, Miroslav Gantar, and Laurie L. Richardson. 2011. “Microcystin Production and Ecological Physiology of Caribbean Black Band Disease Cyanobacteria.” *Environmental Microbiology* 13(4): 900–910.

Sutherland, Kathryn P., James W. Porter, and Cecilia Torres. 2004. “Disease and Immunity in Caribbean and Indo-Pacific Zooxanthellate Corals.” *Marine Ecology Progress Series* 266(Table 1): 273–302.

Wagner, A Ben. 2006. “SciFinder Scholar 2006: An Empirical Analysis of Research Topic Query Processing.”

Wells, O C. 1974. *Scanning Electron Microscopy*. Yorktown Heights, NY: McGraw-Hill.

Zolot, Rachel S, Satarupa Basu, and Ryan P Million. 2013. “Antibody – Drug Conjugates.” *Nature Reviews. Drug Discovery* 12: 259–60.

LIST OF APPENDICES

APPENDIX A: L1 MEDIUM

L1 Medium

Guillard and Hargraves (1993)

This enriched seawater medium is based upon f/2 medium (Guillard and Ryther 1962) but has additional trace metals. It is a general-purpose marine medium for growing coastal algae.

To prepare, begin with 950 mL of filtered natural seawater. Add the quantity of each component as indicated below, and then bring the final volume to 1 liter using filtered natural seawater. The trace element solution and vitamin solutions are given below. Autoclave. Final pH should be 8.0 to 8.2

Component	Stock Solution	Quantity	Molar Concentration in Final Medium
$NaNO_3$	75.00 g L^{-1} dH_2O	1 mL	8.82 x 10^{-4} M
$NaH_2PO_4 \cdot H_2O$	5.00 g L^{-1} dH_2O	1 mL	3.62 x 10^{-5} M
$Na_2SiO_3 \cdot 9H_2O$	30.00 g L^{-1} dH_2O	1 mL	1.06 x 10^{-4} M
Trace element solution	(see recipe below)	1 mL	---
Vitamin solution	(see recipe below)	0.5 mL	---

L1 Trace Element Solution

To 950 mL dH_2O add the following components and bring final volume to 1 liter with dH_2O.

Autoclave.

Component	Stock Solution	Quantity	Molar Concentration in Final Medium
$Na_2EDTA \cdot 2H_2O$	---	4.36 g	1.17×10^{-5} M
$FeCl_3 \cdot 6H_2O$	---	3.15 g	1.17×10^{5} M
$MnCl_2 \cdot 4H_2O$	178.10 g L^{-1} dH_2O	1 mL	9.09×10^{-7} M
$ZnSO_4 \cdot 7H_2O$	23.00 g L^{-1} dH_2O	1 mL	8.00×10^{8} M
$CoCl_2 \cdot 6H_2O$	11.90 g L^{-1} dH_2O	1 mL	5.00×10^{-8} M
$CuSO_4 \cdot 6H_2O$	2.50 g L^{-1} dH_2O	1 mL	1.00×10^{8} M
$Na_2MoO_4 \cdot 2H_2O$	19.90 g L^{-1} dH_2O	1 mL	8.22×10^{-8} M
H_2SeO_3	1.29 g L^{-1} dH_2O	1 mL	1.00×10^{-8} M
$NiSO_4 \cdot 6H_2O$	2.63 g L^{-1} dH_2O	1 mL	1.00×10^{-8} M
Na_3VO_4	1.84 g L^{-1} dH_2O	1 mL	1.00×10^{-8} M
K_2CrO_4	1.94 g L^{-1} dH_2O	1 mL	1.00×10^{-8} M

f/2 Vitamin Solution

(Guillard and Ryther 1962, Guillard 1975)

First, prepare primary stock solutions. To prepare final vitamin solution, begin with 950 mL of dH2O, dissolve the thiamine, add the amounts of the primary stocks as indicated in the quantity column below, and bring final volume to 1 liter with dH2O. At the NCMA we autoclave to sterilize. Store in refrigerator or freezer

Component	Primary Stock Solution	Quantity	Molar Concentration in Final Medium
Thiamine ·HCl (vit. B_1)	---	200 mg	2.96×10^{-7} M
Biotin (vit. H)	0.1 g L^{-1} dH_2O	10 mL	2.05×10^{-9} M
Cyanocobalamin (vit. B_{12})	1.0 g L^{-1} dH_2O	1 mL	3.69×10^{-10} M

APPENDIX B: ANTIMALARIAL ACTIVITY

Table 7. Antimalarial activities of *R. reptotaenium* supernatant and biomass crude extracts as a function of culture duration. The antimalarial potential of bioactive metabolites was evaluated in vitro on a CQ-sensitive strain (*P. falciparum* D6) and a CQ-resistant strain (*P. falciparum* W2). Vero cells (monkey kidney cells) were used to estimate the toxicity of bioactive metabolites. *W2 strain generally shows the same response; exceptions are indicated by parentheses ().*

Type of extracts	Length of culturing	P. falciparum D6 (W2) IC50 (ng/mL)	VERO IC50	P. falciparum D6 (W2) SI
Supernatant crude extracts	2 weeks	19700 (15060)	>47600	>2 (>3)
	3 weeks	1100 (600)	4210	4 (7)
	4 weeks	1160 (970)	>4760	>4 (>5)
	5 weeks	4030 (3090)	>47600	>12 (>15)
	6 weeks	<196	26780	137
	8 weeks	<196	>47600	>243
Biomass crude extracts	2 weeks	27900 (17100)	>47600	>1.7 (>2.8)
	3 weeks	5300	>47600	>9
	4 weeks	5300	>47600	>9
	5 weeks	7700 (6500)	>47600	>6 (>7)
	6 weeks	2500 (4800)	>47600	>19 (>9.9)
	8 weeks	3150 (5500)	>47600	>15 (>8.7)

Table 8. Antimalarial activities of *R. reptotaenium* supernatant and biomass extracts purified by different concentrations of methanol (MeOH) followed by acetone.

Types of extracts	Purified fraction	P. falciparum D6 (W2) IC50 (ng/mL)	VERO IC50 (ng/mL)	P. falciparum D6 (W2) SI
Supernatant extract	Water	NA	4760	NA
	20% MeOH	NA	4760	NA
	40% MeOH	NA	4760	NA
	60% MeOH	3630 (2290)	4760	>1.3 (>2.1)
	80% MeOH	710 (523)	4760	>7 (>9)
	100% MeOH	1.6 (1)	*47.6*	*>30 (>48)*
	100% Acetone	0.33 (0.22)	*47.6*	*>144 (>216)*
Biomass extract	Water	114 (325)	*4760*	>42 (15)
	20% MeOH	114 (325)	4760	>42 (15)
	40% MeOH	4420 (3140)	4760	>1.1 (>1.5)
	60% MeOH	328 (220)	4760	>15 (>22)
	80% MeOH	17 (13)	*476*	*>28 (>37)*
	100% MeOH	2 (2)	*47.6*	*>24 (>24)*
	100% Acetone	15 (6)	476	>32 (>79)

Table 9. Antimalarial activities of *R. reptotaenium* supernatant and biomass extracts purified by different concentrations of acetonitrile followed by acetone

Types of extracts	Purified fractions	P. falciparum D6 (W2) IC50 (ng/mL)	VERO IC50 (ng/mL)	P. falciparum D6 (W2) SI
Supernatant extract	Water	>23800	>23800	1
	20% Acetonitrile	>36890	>36890	1
	40% Acetonitrile	>3570	>3570	1
	60% Acetonitrile	3000 (2160)	>3570	>1.2 (>1.7)
	80% Acetonitrile	480 (412)	>1190	>2.5 (>2.9)
	100% Acetonitrile	2960 (2380)	>3570	>1.2 (>1.5)
	100% Acetone	0.6 (0.5)	567	945 (1134)
Biomass extracts	Water	543 (690)	>23800	>43.8 (>34.5)
	20% Acetonitrile	11400 (1670)	>29750	>2.6 (>17.9
	40% Acetonitrile	>2380	>2380	1
	60% Acetonitrile	2960 (1862)	>3570	>1.2 (1.9)
	80% Acetonitrile	586 (136)	>1190	>2 (>8.7)
	100% Acetonitrile	1097 (180)	>1190	>1.1 (>6.6)
	100% Acetone	10 (19)	>357	>35.7 (>18.6)

Table 10. Bacteria strains isolated from *R. reptotaenium* cultures.

Labrenzia alexandrii	Alphaproteobacteria; Gram (-); Size: 0.5-0.7 x 0.9-3.0μm; rod shape; slightly pink colony; aerobic anoxygenic phototrophs ; salinity: 1-10% NaCl; Biotin and thiamine are required as growth factors; Isolated from cultured cells of the marine dinoflagellate Alexandrrium lusitanicum
Labrenzia aggregata	Alphaproteobacteria; Gram (-); 1.9 um x 0.8 um; rod shape; white to cream colony; obligate aerobic; salinity: 0.3-6%; not require vitamin to grow
Stappia indica	Alphaproteobacteria; Gram (-); 1.0 um x 1.0 um; rod shape; white colony; obligate aerobic; salinity 0.5-11% NaCl; not require vitamin to grow
Koidiimonas gwangyangensis	Alphaproteobacteria; Gram (-); 1.3–1.4 mm x 0.25 mm; rod shape; translucent, creamy white colony; obligate aerobic; optimal NaCl 2%; isolated from Korea
Muricauda aquimarina	Flavobacteria; Gram (-); 0.2–0.5 mm x 2.5–6.0 mm; rod shape; golden yellow colony; aerobic; 1-10% NaCl; isolated from Korea
Phyllobacterium sp.	Alphaproteobacteria; Gram (-); rod shape; transparent colony; aerobic; 1% NaCl

Table 11. Antimalarial activities of metabolites in the extracts of different bacterial strains living in association of *R. reptotaenium* culture.

Types of extracts	Baterial strains	P. falciparum D6 (W2) IC50 (ng/mL)	VERO IC50	P. falciparum D6 (W2) SI
Supernatant extract	*Labrenzia alexandrii*	28000 (37000)	>47600	1.7 (1.2)
	Labrenzia aggregata	>47600	>47600	1
	Kordiimonas sp.	>47600	>47600	1
	Muricauda sp.	44000 (46000)	>47600	>1
	Stappia sp.	>47600	>47600	1
	Phyllobacterium sp.	>47600	>47600	1
	6 bacteria growing together	>47600	>47600	1
Biomass extracts	*Labrenzia alexandrii*	>47600	>47600	1
	Labrenzia aggregata	>47600	>47600	1
	Kordiimonas sp.	>47600	>47600	1
	Muricauda sp.	>47600	>47600	1
	Stappia sp.	>47600	>47600	1
	Phyllobacterium sp.	>47600	>47600	1
	6 bacteria growing together	>47600	>47600	1

Table 12. Antimalarial activities of different parts of the active fractions (supernatant-acetone 100%)

Parts	P. falciparum D6 (W2) IC50 (ng/mL)	VERO IC50 (ng/mL)	P. falciparum D6 (W2) SI
0-2.5 min	>1190	>1190	1
2.5-4.5 min	<4.9	587.8	120
4.5-9.0 min	156.1 (108.6)	>1190	>7.6 (>11)
9.0-12.0 min	>1190	>1190	1
Combination	25 (13.8)	>1190	>47.6 (>86.5)

Table 13. The relative abundance (%) of major bacterial phyla and subphyla in *R. reptotaenium* 2 weeks-old and 8 weeks-old culture.

	% composition of the whole community	
	2 weeks	8 weeks
Bacteroidetes	13.2	17.8
Rhodothermi	7.8	9.1
Saprospirae	0.9	3.7
Cytophagia	4.0	3.4
Flavobacteriia	0.6	1.6
Cyanobacteria	7.6	4.1
Oscillatoriophycideae	7.6	4.1
Planctomycetes	12.7	15.2
Phycisphaerae	3.5	2.1
Planctomycetia	9.2	13.1
Proteobacteria	60.4	55.0
Alphaproteobacteria	58.6	52.9
Betaproteobacteria	0.1	0.1
Gammaproteobacteria	1.6	2.1
Other	6.1	7.9
Total	100	100

VITA

Thuy Nguyen was born in Ho Chi Minh city, Vietnam. She got a B.S. in Biotechnology in CanTho Univeristy, Vietnam. She pursued her M.S. degree with Dr. Hom at the University of Mississippi (UM) with the support of a Vietnam Education Foundation (VEF) Fellowship. She worked in the collaboration project between the Bigelow Lab (Maine), the National Center for Natural Products Research, and the Hom lab. Her research interests focus on harmful algal bloom and the natural products derived from marine algae. She graduated with a M.S. in Biology in August 2017, after which she pursued work in understanding the secondary metabolite production of toxic marine algae.